

**ISTANBUL TECHNICAL UNIVERSITY ★ GRADUATE SCHOOL OF SCIENCE**  
**ENGINEERING AND TECHNOLOGY**

**MULTIFUNCTIONAL FORMATE DEHYDROGENASE FUSION PROTEIN  
BINDS TO GOLD SURFACE WITH IMPROVED REACTION KINETICS**

**M.Sc. THESIS**

**Deniz Tanıl YÜCESOY**

**Department of Advanced Technologies**

**Molecular Biology Genetics and Biotechnology Programme**

**DECEMBER 2011**



**ISTANBUL TECHNICAL UNIVERSITY ★ GRADUATE SCHOOL OF SCIENCE**  
**ENGINEERING AND TECHNOLOGY**

**MULTIFUNCTIONAL FORMATE DEHYDROGENASE FUSION PROTEIN  
BINDS TO GOLD SURFACE WITH IMPROVED REACTION KINETICS**

**M.Sc. THESIS**

**Deniz Tanıl YÜCESOY**  
**(521091085)**

**Department of Advanced Technologies**

**Molecular Biology Genetics and Biotechnology Programme**

**Thesis Advisor: Assoc. Prof. Dr. Ayten KARATAŞ**  
**Co-Advisor: Prof. Dr. Candan TAMERLER**

**DECEMBER 2011**



**İSTANBUL TEKNİK ÜNİVERSİTESİ ★ FEN BİLİMLERİ ENSTİTÜSÜ**

**ALTIN YÜZEYE BAĞLANABİLEN ÇOK YÖNLÜ FORMAT  
DEHİDROGENAZ FÜZYON PROTEİNİNİN GELİŞTİRİLMİŞ KİNETİK  
AKTİVİTESİ**

**YÜKSEK LİSANS TEZİ**

**Deniz Tanıl YÜCESOY  
(521091085)**

**İleri Teknolojiler Anabilim Dalı**

**Moleküler Biyoloji Genetik ve Biyoteknoloji Programı**

**Tez Danışmanı: Doç. Dr. Ayten KARATAŞ  
Eş Danışmanı: Prof. Dr. Candan TAMERLER**

**ARALIK 2011**



**Deniz Tanıl Yücesoy**, a **M.Sc.** student of **ITU Graduate School of Science Engineering and Technology** student ID **521091085**, successfully defended the thesis entitled “**MULTIFUNCTIONAL FORMATE DEHYDROGENASE FUSION PROTEIN BINDS TO GOLD SURFACE WITH IMPROVED REACTION KINETICS**”, which he prepared after fulfilling the requirements specified in the associated legislations, before the jury whose signatures are below.

**Thesis Advisor :**     **Assoc. Prof. Dr. Ayten KARATAŞ**                     .....  
İstanbul Technical University

**Co-advisor :**           **Prof.Dr. Candan TAMERLER**                     .....  
İstanbul Technical University

**Jury Members :**       **Assoc. Prof. Dr. Nevin Gül KARAGÜLER**.....  
İstanbul Technical University

**Assoc. Prof. Dr. Zeynep Petek ÇAKAR**                     .....  
İstanbul Technical University

**Assist. Prof. Dr. Şermin Utku**                                     .....  
Tekirdağ Namık Kemal University

**Date of Submission : 9 December 2011**

**Date of Defense : 20 December 2011**





*To my family,*



## FOREWORD

I first would like to thank my thesis supervisors, Prof. Dr. Candan Tamerler and Assoc. Dr. Ayten Karataş, for their support and guidance during the preparation of this thesis. I also would like to thank Assoc. Prof. Dr. Nevin Gül Karagüler for her mentoring throughout the project. Their guidance and comments created the scope and quality of this thesis.

I would like to thank my friend Sibel Çetinel for the support she had provided during my studies. This study would not be such enjoyable without her.

Many thanks to my lab mate and my dear friend Burak Çalışkan for sharing his ideas and helping throughout the project.

I also thank all faculty members contributing to the program. They made my two years in this program an exciting intellectual journey.

Many thanks to my dear friends for their support during two years. I always had continuous support from my friends Gökhan Küçükgoze, Nurcan Vardar, İrem Avcılar, Süha Akan and Şerif Karabulut.

I also would like to thank everybody in MOBGAM. I really enjoyed sharing same workplace with them.

I am always grateful to my mother, father, brother and sister for their love, encouragement and support throughout my whole life. But, I would like to thank my father specially for teaching me the value and joy of science in my childhood.

And finally, thank you Duygu for all the love and happiness you brought into my life. Many thanks for the cake and the coffee as well. It was the nicest reward I had in my life for being a hard-working ☺ student.

December 2011

Deniz Tanıl YÜCESOY



## TABLE OF CONTENTS

	<u>Page</u>
<b>FOREWORD</b> .....	<b>ix</b>
<b>TABLE OF CONTENTS</b> .....	<b>xi</b>
<b>ABBREVIATIONS</b> .....	<b>xiii</b>
<b>LIST OF TABLES</b> .....	<b>xv</b>
<b>LIST OF FIGURES</b> .....	<b>xvii</b>
<b>SUMMARY</b> .....	<b>xix</b>
<b>ÖZET</b> .....	<b>xxi</b>
<b>1. INTRODUCTION</b> .....	<b>1</b>
1.1 Purpose of Thesis .....	1
1.2 NAD <sup>+</sup> -Dependent Formate Dehydrogenase .....	1
1.2.1 Overview of NAD <sup>+</sup> -dependent formate dehydrogenase .....	1
1.2.2 Catalytic properties of NAD <sup>+</sup> -dependent formate dehydrogenase .....	6
1.2.3 Structural properties of NAD <sup>+</sup> -dependent formate dehydrogenase .....	7
1.2.4 Industrial applications of NAD <sup>+</sup> -dependent formate dehydrogenase .....	8
1.3 Protein Immobilisation Strategies .....	9
1.3.1 Physical adsorption .....	9
1.3.2 Covalent immobilisation .....	10
1.3.2.1 Amine chemistry .....	11
1.3.2.2 Thiol chemistry .....	12
1.3.2.3 Carboxyl chemistry .....	13
1.3.2.4 Photoactive chemistry .....	13
1.3.2.5 Peptide ligation .....	14
1.3.3 Affinity .....	14
1.3.3.1 Avidin-biotin system .....	15
1.3.3.2 Polyhistidine-tag system .....	16
1.3.3.3 Protein A/ protein G-mediated immobilisation .....	17
1.3.4 Protein immobilisation strategies .....	18
1.3.4.1 Gold nanoparticles .....	19
1.3.4.2 Carbon nanotubes .....	19
1.3.4.3 Magnetic nanoparticles .....	20
1.3.4.4 Porous silica structures .....	20
1.4 Genetically Engineered Peptides for Inorganics (GEPI) .....	21
1.4.1 Combinatorial methods for selecting first generation GEPI's .....	21
1.4.2 Computational biomimetics for further characterization of GEPIs .....	23
1.4.3 GEPI as a bifunctional immobilisation tool .....	24
1.5 Surface Plasmon Resonance (SPR) Spectroscopy .....	25
<b>2. MATERIALS AND METHODS</b> .....	<b>27</b>
2.1 Materials .....	27
2.1.1 Laboratory equipments .....	27
2.2 Methods .....	27

2.2.1 AuBP2 selection.....	27
2.2.2 AuBP2-FDH fusion protein construction.....	27
2.2.3 Protein expression.....	31
2.2.4 Protein purification.....	32
2.2.5 Histidine tag removal.....	32
2.2.6 Kinetic activity assay.....	33
2.2.7 Binding kinetics assay.....	33
<b>3. RESULTS AND DISCUSSION.....</b>	<b>35</b>
3.1 Gold Binding Peptide (AuBP) Selection and Characterization.....	35
3.2 AuBP2-FDH Fusion Protein Construction.....	37
3.3 Protein Expression.....	40
3.4 Protein Purification.....	40
3.5 Histidine Tag Removal.....	42
3.6 Kinetic Activity of AuBP2-FDH.....	43
3.7 Binding Kinetics of wt-FDH and AuBP2-FDH.....	46
<b>4. CONCLUSIONS AND FUTURE PERSPECTIVES.....</b>	<b>49</b>
<b>REFERENCES.....</b>	<b>53</b>
<b>APPENDICES.....</b>	<b>59</b>
<b>CURRICULUM VITAE.....</b>	<b>65</b>

## ABBREVIATIONS

<b>AuBP2</b>	: Gold Binding Protein
<b>GEPI</b>	: Genetically Engineered Peptides for Inorganics
<b><i>cb</i>FDH</b>	: <i>Candida boidinii</i> Formate Dehydrogenase
<b><i>cm</i>FDH</b>	: <i>Candida methylica</i> Formate Dehydrogenase
<b>EDTA</b>	: Ethylenediaminetetraaceticacid
<b>IPTG</b>	: Isopropyl-Beta-D-Thiogalactopyranoside
<b>LB</b>	: Luria-Bertani Broth (Lysogeny Broth)
<b>NAD<sup>+</sup></b>	: Nicotinamide Adenine Dinucleotide
<b>NADP</b>	: Nicotinamide Adenine Dinucleotide Phosphate
<b>OD</b>	: Optical Density
<b>RT</b>	: Room Temperature
<b>SPR</b>	: Surface Plasmon Resonance
<b>uRIU</b>	: Micro Refractive Index Unit
<b><i>sc</i>FDH</b>	: <i>Saccharomyces cerevisiae</i> Formate dehydrogenase
<b>SOC</b>	: Super Optimal Broth with Catabolite Repression





## LIST OF TABLES

	<u>Page</u>
<b>Table 1.1</b> : Important mutations in NAD <sup>+</sup> -dependent FDH .....	4
<b>Table 1.2</b> : Active sites for covalent attachment.....	10
<b>Table 1.3</b> : Application of protein immobilisation .....	18
<b>Table 2.1</b> : Primer sequences used in fusion protein construction .....	27
<b>Table 2.2</b> : PCR Conditions (1st Step) used in fusion protein construction.....	28
<b>Table 2.3</b> : PCR Conditions (2nd Step) used in fusion protein construction. ....	29
<b>Table 2.4</b> : BigDye Terminator v3.1 cycle sequencing PCR .....	30
<b>Table 2.5</b> : Primer sequences of site-directed mutagenesis reaction. ....	31
<b>Table 3.1</b> : Amino acid sequences, MW, pI, and net charges of selected peptides ...	35
<b>Table 3.2</b> : The resulting kinetic constants of selected peptides. ....	36
<b>Table 3.3</b> : Fusion protein constructs and expected molecular weights.....	37
<b>Table 3.4</b> : Activity constants of wt-FDH and AuBP2-FDH .....	46
<b>Table 3.5</b> : Binding constants of wt-FDH and AuBP2-FDH.....	46



## LIST OF FIGURES

	<u>Page</u>
<b>Figure 1.1</b> : NAD(P) regeneration system.....	3
<b>Figure 1.2</b> : Cartoon display of <i>cb</i> FDH. ....	8
<b>Figure 1.3</b> : Reaction of FDH employed in industry. ....	9
<b>Figure 1.4</b> : Amine chemistry on NHS-derivatized surface. ....	11
<b>Figure 1.5</b> : Aldehyde-derivatized surfaces]. ....	11
<b>Figure 1.6</b> : Maleimide-derivatized thiol chemistry on surfaces. ....	12
<b>Figure 1.7</b> : Disulfide-derivatized thiol chemistry on surfaces. ....	12
<b>Figure 1.8</b> : Vinyl sulfone-derivatized thiol chemistry on surfaces.....	12
<b>Figure 1.9</b> : Carboxyl chemistry using carbodiimide activation. ....	13
<b>Figure 1.10</b> : Peptide ligation. ....	14
<b>Figure 1.11</b> : Glycopolymer-derivatized surface via a biotin-streptavidin layer. ....	16
<b>Figure 1.12</b> : Binding of His-tagged proteins on a Ni-NTA surface. ....	17
<b>Figure 1.13</b> : Antibody immobilization using a layer-by-layer architecture.....	17
<b>Figure 1.14</b> : Schematic fabrication of mesoporous silica nanoparticles.....	20
<b>Figure 1.15</b> : Insertion site of the random peptide library in cell surface display system. ....	22
<b>Figure 1.16</b> : Schematic view of cell surface display and phage display methods....	23
<b>Figure 1.17</b> : Knowledge based approach in generating next generation of peptides with superior binding properties. ....	24
<b>Figure 3.1</b> : Schematic presentation of AuBP2-FDH fusion protein.....	38
<b>Figure 3.2</b> : Agarose gel.....	39
<b>Figure 3.3</b> : Agarose gel.....	39
<b>Figure 3.4</b> : SDS gel picture of wtFDH .....	41
<b>Figure 3.5</b> : SDS gel picture of AuBP2-FDH.....	41
<b>Figure 3.6</b> : Velocity vs substrate concentration graph of wt-FDH.....	44
<b>Figure 3.7</b> : (1/V) vs. (1/S) graph of wt-FDH .....	44
<b>Figure 3.8</b> : Velocity vs substrate concentration graph of AuBP2-FDH .....	45
<b>Figure 3.9</b> : (1/V) vs. (1/S) graph of AuBP2-FDH .....	45
<b>Figure 3.10</b> : SPR sensogram of wt-FDH .....	47
<b>Figure 3.11</b> : SPR sensogram of AuBP2-FDH.....	47
<b>Figure 3.12</b> : Surface display of <i>cb</i> FDH. ....	48



## MULTIFUNCTIONAL FORMATE DEHYDROGENASE FUSION PROTEIN BINDS TO GOLD SURFACE WITH IMPROVED REACTION KINETICS

### SUMMARY

NAD<sup>+</sup>-dependent formate dehydrogenases (EC 1.2.1.2, FDH) belonging to superfamily of D-specific 2-hydroxy acid dehydrogenases plays an important role in the energy supply mechanisms of methylotrophic microorganisms. FDHs mainly catalyze the oxidation of formate ion to CO<sub>2</sub> where the reaction coupled with the reduction of NAD<sup>+</sup> to NADH. As a result, a single C-H bond in the substrate breaks down and a new C-H bond in the NADH forms. NAD<sup>+</sup>-dependent FDHs are versatile biocatalysts in the enzymatic synthesis of valuable optically active chiral compounds in the industry. However, the yield of the reaction is too low due to the laborious purification steps. Moreover, chemical immobilization methods cause a sharp decrease in the activity of enzyme. Controlled binding and assembly of proteins onto inorganic substrates are at the core of bio-nanotechnology. Genetically engineered peptides for inorganics (GEPI) provide molecular linkage between the proteins and inorganic surfaces. GEPI-mediated immobilization techniques do not have such drawbacks that chemical immobilization methods have like random orientation of proteins on solid surfaces and multi-step chemical reactions requirements. Moreover, GEPIs have certain benefits like ability to work in physiological conditions and enhanced functional durability. The aim of this study is to construct fusion protein by attaching the biocombinatorially selected Gold Binding Peptide (AuBP2) to the N-terminal of *Candida methylica* FDH enzyme (*cmFDH*) and characterize the multifunctional properties, and finally demonstrate the effects of AuBP2 conjugation on binding and kinetic properties of FDH enzyme on both soluble and immobilized forms on the gold surface. With this purpose, AuBP2-FDH fusion enzyme has successfully cloned and expressed. Purification of both fusion and wild type enzymes performed. Then, kinetic and binding characteristics were calculated. Data showed that AuBP2 addition to the enzyme did not make a significant change in the kinetic parameters of the FDH enzyme but cause 12-fold increase in adsorption behavior of enzyme on gold surface, which demonstrates that gold specific AuBP2 peptide, is an ideal linker molecule for FDH immobilization on gold surface.



## ALTIN YÜZEYE BAĞLANABİLEN ÇOK YÖNLÜ FORMAT DEHİDROGENAZ FÜZYON PROTEİNİNİN GELİŞTİRİLMİŞ KİNETİK AKTİVİTESİ

### ÖZET

NAD<sup>+</sup>-bağımlı format dehidrogenaz (EC 1.2.1.2, FDH) enzimi, format iyonlarını CO<sub>2</sub> 'ye yükseltgeyip aynı zamanda NAD<sup>+</sup> molekülünü NADH'a indirgeyen değerli bir enzimdir.

D-özgü 2- hidroksi asit dehidrogenaz süper familyasına ait olan bu enzim, aileye mensup diğer enzimlerden yapısal ve substrat ilgisi bakımından bir takım farklılıklar içermektedir. FDH enziminin katalizlediği reaksiyonun diğer dehidrogenazlara oranla oldukça basit olması ve tek basamaklı olması sebebiyle, enzim endüstriyel ve bilimsel kullanımda oldukça yaygındır.

NAD<sup>+</sup>-bağımlı format dehidrogenaz enzimi ilk olarak 1950'li yıllarda Mathews tarafından bezelye tohumlarından elde edilmiştir. Buna karşılık enzim popülarlığını 1970'li yılların sonunda kiral moleküllerin endüstriyel sentezinde kullanılan kofaktörlerin geri dönüştürülmesi ve tekrar tekrar kullanılması amacıyla oluşturulan biyoreaktörde kullanılması ile kazanmıştır.

2000'li yılların başında gelişen DNA dizi analizi teknolojisi sayesinde birçok farklı organizmada NAD<sup>+</sup>-bağımlı format dehidrogenaz genleri tanımlanmıştır. Bu organizmalar arasında en çok ilgiyi içerdikleri FDH enziminin dayanıklılığı ve yüksek kinetik aktivitesinden dolayı *Candida* cinsine ait organizmalar çekmiştir.

Tüm bu çalışmalar ışığında NAD<sup>+</sup>-bağımlı format dehidrogenaz enziminin hücre içinde çeşitli stres durumlarında arttığı ve bir çeşit anti-stres proteini olarak görev alıyor olabileceği düşünülmüş ve bu alanda çalışmalara hız verilmiştir.

FDH enziminin kofaktör geri dönüşümünde kullanılan en etkili enzim olmasının başlıca sebepleri arasında ilk olarak enziminin katalizlediği reaksiyonun geri dönüşümsüz olması, buna bağlı ikincil reaksiyonun tek yönde ilerlemesi ve bu sayede % 100'e yakın bir verim elde edilmesi gösterilebilir. Buna ek olarak FDH enziminin katalizlediği reaksiyonun son ürününün CO<sub>2</sub> olması ve CO<sub>2</sub>'in kolayca buharlaşması sayesinde ekstra saflaştırma adımlarına gerek duyulmaz. Ayrıca, uygun çalışma pH aralığı 6.0-9.0 olması sayesinde de farklı enzimlerle kullanımı mümkündür. Son olarak metanolü karbon kaynağı olarak kullanan mikroorganizmalarda üretilebilmesi sayesinde üretim maliyeti oldukça düşüktür.

Tüm bu faktörler ışığında Bommarius ve öğrencileri 1995 yılında *Candida boidinii* mikroorganizmasından izole ettikleri NAD<sup>+</sup>-bağımlı format dehidrogenaz enzimini L-tert-leucine amino asidinin kiral sentezinde kofaktör geri kazanımı amacıyla başarılı bir şekilde kullanmışlardır.

NAD<sup>+</sup>-bağımlı format dehidrogenaz enziminin başlıca dezavantajları arasında aktif sistein amino asitlerinden kaynaklanan düşük dayanıklılığı, NADP kofaktör molekülüne özgü ilgisinin olmaması ve üretildiği metanol kullanan mikroorganizmaların yüksek maliyetidir. Tüm bu dezavantajların üstesinden

gelebilmek amacıyla protein mühendisliği yöntemleri kullanılarak enzim üzerinde çeşitli modifikasyonlar ve mutasyonlar yaratılmıştır.

NAD<sup>+</sup>-bağımlı format dehidrogenaz enzimi doğrudan hidrit iyonu (H<sup>-</sup>) transferini gerçekleştirebilme kabiliyetine sahip olduğundan bu az görülen reaksiyonunun çalışılabilmesi ve tepkime basamaklarının aydınlatılabilmesi açısından da son derece uygun bir enzimdir.

NAD<sup>+</sup>-bağımlı format dehidrogenaz enzimi genel olarak çift substratlı sıralı Bi-Bi reaksiyonu mekanizması ile çalışır. Bu mekanizmada NAD<sup>+</sup> molekülü birincil substrat olarak görev alır ve enzime bağlanması, enzimin formata iyonuna olan ilgisini üç kat artırır. Bu reaksiyon türü dehidrogenazların önemli bir kısmında da oldukça yaygındır.

NAD<sup>+</sup>-bağımlı format dehidrogenaz enzimi amino ve karboksil bölgeleri olmak üzere iki ana bölüme ayrılabilir. Amino bölgesinin enzim aktivitesinde önemli bir role sahip olduğu bilinmektedir. Maya ve mantar kökenli NAD<sup>+</sup>-bağımlı format dehidrogenaz enzimlerinin amino asit dizilerinde herhangi bir fark olmamasına rağmen, bakteriyel kökenli NAD<sup>+</sup>-bağımlı format dehidrogenaz enziminde bir takım amino asit eklenmeleri mevcuttur.

*Candida methylica* NAD<sup>+</sup>-bağımlı format dehidrogenaz enzimi yaklaşık olarak 46000 Dalton boyutunda ve 364 amino asitten oluşan bir moleküldür. Yapılan çalışmalarda ayrıca *Candida methylica* NAD<sup>+</sup>-bağımlı format dehidrogenaz (*cmFDH*) ve *Candida boidini* NAD<sup>+</sup>-bağımlı format dehidrogenaz (*cbFDH*) NAD<sup>+</sup>-bağımlı format dehidrogenaz enzimlerinin katalitik bölgesindeki amino asitlerin aynı oldukları görülmüştür. Bunlar, 77. sıradaki Prolin (Pro77), 78. sıradaki Fenilalanin (Phe78), 102. sıradaki İzolösin (Ile102), 118. sıradaki Asparajin (Asn118), 171. sıradaki Alanin veya Glisin (Ala/Gly171), 173. sıradaki Glisin (Gly173), 176. sıradaki Glisin (Gly176), 267. sıradaki Arjinin (Arg267), 287. sıradaki Glütamin (Gln287) ve 310. sıradaki Histidin (His310) amino asitleridir.

FDH enzimi endüstride oldukça yaygın kullanım alanına sahiptir. Bunların başında kiral moleküllerin sentezi gelir. Nikotinamid adenin dinükleotid kullanımından doğan yüksek maliyeti azaltabilmek amacıyla bu tür üretimlerde FDH enzimi NADH indirgeni olarak kullanılır. Diğer bir kullanım alanı ise format biyosensörleridir. Format biyosensörlerinde, format iyonunun varlığını eser miktarda da olsa tanımlayabildiği için, sensör uygulamalarında oldukça yaygın olarak kullanılır.

Nikotinamid adenin dinükleotid (NAD) yaklaşık olarak 300'den fazla dehidrogenaz enzimi tarafından kofaktör olarak kullanılan ve elektrokatalitik yükseltgenmesi sonucu katı yüzey üzerinde yüksek bir potansiyel fark meydana getiren bir moleküldür. Bu enzimlerin farklı substratlar varlığında NADH'a olan özgülüklerinin artırılması ve redoks kabiliyetlerinin yükseltilmesi üzerine uygulanan analitik yaklaşımlar ve çalışmalar literatürde mevcuttur.

Enzimlerin endüstriyel alanda tekrar tekrar kullanılabilmesi, dayanıklılığının artırılması amacıyla günümüze kadar çeşitli tutuklama yöntemleri geliştirilmiştir. Literatürde birçok farklı tutuklama metodu mevcuttur. Bunların arasında elektriksel etkileşim aracılığı ile fiziksel tutuklama ve kovalent bağ oluşturup kimyasal olarak bağlama yöntemleri en geniş yeri kaplar. Özellikle kovalent bağ oluşturup kimyasal olarak bağlama yöntemi için literatürde onlarca farklı yaklaşım mevcuttur. Bunların arasında ilk olarak akla gelenler, amin, tiyol, karboksil reaksiyonlarıdır. Son zamanlarda ise bu söz konusu geleneksel tutuklama yöntemleri sebep olduğu çeşitli sorunlar nedeniyle yerlerini daha modern metotlara bırakmışlardır. Elektriksel etkileşim ile fiziksel tutuklama metodunda bağın zayıflığından doğan akma problemleri ve kovalent bağ ile tutuklama metodunda sıklıkla görülen enzimin



kinetik aktivitesindeki azalma bu problemlere başlıca örneklerdir. Tutuklama için kullanılabilen bir diğer yol ise biyomoleküllerin birbirine olan ilgisine dayalı histidin kuyruğu ve biyotin-avidin etkileşimi yöntemleridir. Fakat bu yöntemler de birtakım sorunlar içermektedirler.

Gen mühendisliği yöntemiyle geliştirilmiş olan (GEPI) peptitler farklı inorganik yüzeylere özgün olarak bağlanabilme kapasitesine sahiptir. Bu dizilerin inorganik malzemelere olan seçici ve yüksek ilgisi enzim tutuklama teknolojisinde geleneksel metodlara iyi bir alternatif olacağı düşünülmüştür.

Bu amaçla FDH enziminin amino ucuna altın yüzeylerine özgün bağlanan peptit dizisi (AuBP2) eklenmiş ve birlikte füzyon halinde üretilmesi sağlanmıştır. Peptitin boyunun uzun olması sebebiyle eklenmesi beş farklı primer ve iki farklı PCR reaksiyonu ile gerçekleştirilmiştir. Sonrasında peptit-enzim füzyonlarının *E. coli* bakteriyel ekspresyon sisteminde, güçlü bir promotor altında IPTG indüklenmesi vasıtasıyla üretilmeleri sağlanmıştır. Enzimin içerdiği Histidin amino asitlerinden oluşan kuyruğun Nikel Nitriлотriasetik asit molekülüne (Ni-NTA) olan ilgisi kullanılarak saflaştırılması gerçekleştirilmiştir.

Saflaştırılan proteinler sodyum dodesil sülfat poliakrilamid jel elektroforezi (SDS-PAGE) ile görüntülenmiş ve yeterli saflıkta elde edildiklerini belirlenmiştir.

Saflaştırma aracı olarak kullanılan enzimin amino ucunda yer alan altı adet Histidin amino asidi altına özgül olmayan şekilde bağlanma kapasitesine sahip olduklarından dolayı PreScission Proteaz enzimi vasıtası ile uzaklaştırılmıştır. Histidin kuyruğu denilen bu bölge saflaştırılmış enzimlerden uzaklaştırıldıktan sonra aktivite tayinleri literatürde varolan yöntemler uygulanarak yapılmıştır. Bu amaçla, format iyonunun substrat olarak kullanıldığı ve  $NAD^+$  kofaktörü aracılığı ile gerçekleşen reaksiyon koşulları literatürde belirtilen koşullarda hazırlanmış ve değişen format iyonu konsantrasyonunda oluşan NADH molekülü tayini 340 nanometre dalga boyunda UV-spektrofotometresi kullanılarak yapılmıştır. Elde edilen sonuçlar ışığında, amino ucuna altın yüzeylerine özgün bağlanan peptit dizisi (AuBP2) eklenen  $NAD^+$ -bağımlı format dehidrogenaz enziminin kinetik aktivite değerlerinde altın yüzeylerine özgün bağlanan peptit dizisi (AuBP2) eklenmemiş  $NAD^+$ -bağımlı format dehidrogenaz enzimine oranla herhangi bir azalma olmadığı gözlemlenmiştir.

Sonrasında yüzey plasmon rezonans spektroskopisi (SPR) yöntemiyle oluşturduğumuz füzyon proteininin altın kaplı SPR yüzeylerinde tutuklama kapasitesi ölçülmüş ve AuBP2 eklenmemiş  $NAD^+$ -bağımlı format dehidrogenaz enzimi ile karşılaştırılmıştır. Bu sonuçlar ışığında da amino ucuna altın yüzeylerine özgün bağlanan peptit dizisi (AuBP2) eklenen  $NAD^+$ -bağımlı format dehidrogenaz enziminin, AuBP2 eklenmemiş  $NAD^+$ -bağımlı format dehidrogenaz enzimine oranla altın yüzeye 12 kat daha güçlü bağlandığı tayin edilmiştir.

Sonuç olarak tüm bu veriler ışığında AuBP2 peptidinin enzim aktivitesinde herhangi bir azalmaya yol açmadığı buna karşılık enzime altın yüzeye özgün şekilde bağlanabilme yeteneği kazandırdığı gösterilmiş ve bu amaçla enzimlere eklenebilecek ideal bir molekül olduğu ispatlanmıştır.



## 1. INTRODUCTION

### 1.1 Purpose of Thesis

Oriented enzyme immobilization is a major challenge and the primary aim of this project is to develop multifunctional enzyme that can immobilized on the inorganic material surface at a close proximity for a variety of applications.

Due to industrial importance, in this project we focus on developing a novel immobilization method for format dehydrogenase enzyme on a gold surface.

The specific purpose of this project is to construct Gold Binding Peptide (AuBP2)-NAD<sup>+</sup>-dependent formate dehydrogenase (AuBP2-FDH) fusion enzyme and characterize its multifunctional properties, and finally demonstrate the effects of AuBP2 peptide conjugation on binding and kinetic properties of FDH enzyme on both soluble and immobilized forms on the gold surface.

### 1.2 NAD<sup>+</sup>-Dependent Formate Dehydrogenase

#### 1.2.1 Overview of NAD<sup>+</sup>-dependent formate dehydrogenase

NAD<sup>+</sup>-dependent formate dehydrogenase (EC 1.2.1.2, FDH) is a valuable enzyme that mainly catalyzes the oxidation of formate ion into carbon dioxide (CO<sub>2</sub>) coupled to the reduction of NAD<sup>+</sup> to NADH. The one-step reaction mechanism is formulated below (1.1).



FDH belongs to the superfamily of D-specific 2- hydroxy acid dehydrogenase. Members of this D-specific 2- hydroxy acid dehydrogenase superfamily mainly varied in terms of their quaternary structures, type of prosthetic groups they contain, and their substrate specificities. The choice of FDH as a model enzyme was based on the fact that the enzyme catalyzes the simplest reaction among other enzymes of the superfamily devoid of any proton release or abstraction steps [1, 2].

The NAD<sup>+</sup>-dependent formate dehydrogenases enzyme was first isolated from pea seeds in 1950, but it was late 1970's when the enzyme attracted researchers and studies about its catalytic properties and potential applications began. The interest originated from its practical application for the purposes of NADH regeneration in the enzymatic processes of chiral synthesis [3, 4]. In literature, significant number of studies about formate dehydrogenase enzymes is from methylotrophic bacteria and yeast origin.

By the advances in high throughput genome sequencing technologies during the last few decades, new FDH genes discovered in various organisms including pathogens such as *Staphylococcus aureus* [5], *Mycobacterium avium* subspecies [6], different strains of *Bordetella* [7] and *Legionella* [8, 9], *Francisella tularensis* subspecies [7], *Histoplasma capsulatum* [10], *Cryptococcus neoformans* JEC21 [11], *Pseudomonas* sp.101, *Moraxella C-2*, *Saccharomices cerevisiae*, *Hansenula polymorpha*, *Candida methylica*, *Candida boidinii*, fungi *Aspergillus nidulans*, *Neurospora crassa*, potato mitochondria and barley [1, 2, 12, 13]. Parts of FDH genes are present in mammals, e.g. mouse (GeneBank Accession AA681620) and human (GeneBank Accession N75707) as well.

Among the large number of microorganism containing NAD<sup>+</sup>-dependent formate dehydrogenase genes, the greatest attention gained by the discovery of NAD<sup>+</sup>-dependent formate dehydrogenase homologs in yeasts. *Candida* species among these various methanol consuming yeast species showed that they are the best candidate for NAD<sup>+</sup>-dependent formate dehydrogenase isolation due to their stability and relatively high activity [14].

As a consequence of these studies, it was seen that FDH plays a key role in cell functioning under certain conditions. FDH localizes in mitochondria and its biosynthesis dramatically increases under stress conditions in plants [1]. For example, in 1999, Weerasinghe and his colleagues conducted a study with the aim of identifying unhealthy trees by analyzing the ratio of FDH isoforms [15]. Moreover, in *Staphylococcus aureus*, FDH is one of three overexpressed proteins, during biofilm formation [16]. It was also seen that the expression of FDH genes is phase specific in fungal pathogens [10]. The number of studies on FDH grows year by year, and nowadays a significant number of studies are about biotechnological

applications of FDH in the processes of chiral synthesis with  $\text{NAD(P)}^+$ -dependent oxidoreductases. General scheme of  $\text{NAD(P)}$  regeneration for cofactor coupled enzymatic synthesis of optically active compounds is presented in Figure 1.1 below:

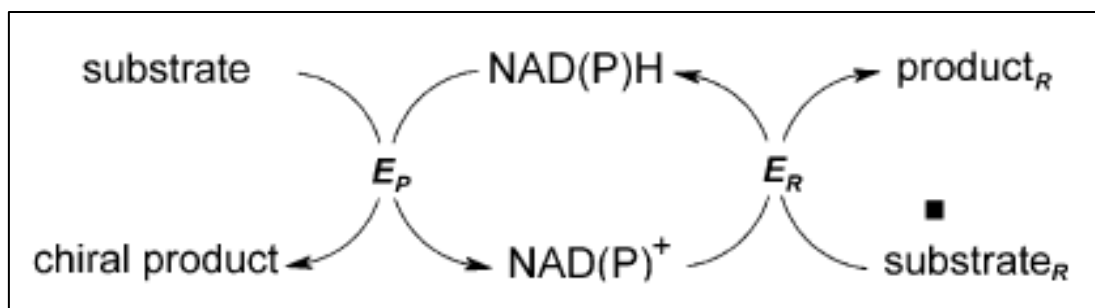


**Figure 1.1** :  $\text{NAD(P)}$  regeneration system [1].

In Figure 1.1 above, the main enzyme  $E_P$  (dehydrogenase, reductase, monooxygenase, etc.) catalyzes production of a chiral compound using reduced cofactor, while the second enzyme  $E_R$  (for example, formate dehydrogenase) reduces oxidized coenzyme back to  $\text{NAD(P)H}$ . In some cases, the same enzyme can catalyze both reactions [3, 17]. Numerous studies demonstrated that FDH is one of the best enzymes for the purposes of reduced cofactor [1, 3, 18].

The significance of the reaction that is catalyzed by FDH is based on several features of enzyme which provides certain benefits. First of all, the reaction that is catalyzed by FDH is irreversible which provides thermodynamic pressure and results in a 99–100% yield of the final product by shifting equilibrium of main reaction. Secondly, formate ion, the primary substrate of reaction, is cheap and reaction product is only  $\text{CO}_2$  that can easily remove from the reaction. Furthermore, the optimum working pH range of FDH is between 6.0–9.0 which makes it suitable for multienzyme reactions. Moreover, production costs of FDH enzyme in methanol-utilizing yeasts and bacteria is relatively low. FDHs produced in methanol-utilizing yeasts and bacteria are stable enough to employ in flow-through reactors for a while, as well. By taking into account of all these factors, Bommarius and his colleagues purified FDH enzyme from *Candida boidinii* and used it in the process of chiral synthesis of L-tert-leucine coupled with dehydrogenases with the purpose of  $\text{NADH}$  regeneration [19].

To provide a more powerful biocatalyst from a practical viewpoint and to overcome certain limitations of native FDH, such as its low operational stability due to the

presence of active cysteine (Cys) residues, lack of NADP<sup>+</sup> cofactor specificity, and high production cost of native strains of methylotrophic bacteria or yeast, wild-type FDH was subjected to several directed evolution cycles and protein engineering studies [1].

Most of these protein engineering studies in literature have focused on improving kinetic properties, increasing its chemical and thermal stability, switching its coenzyme specificity, optimizing and enhancing the level and rate of FDH gene expression in *Escherichia coli* (*E. coli*). Some of the important mutations listed in Table 1.1 below.

**Table 1.1** : Important mutations in NAD<sup>+</sup>-dependent FDH [1].

<b>Aim</b>	<b>Mutation/source</b>	<b>Result/conclusion</b>
Probing of molecular mechanism Increase of specific activity	C23S/F285S <i>Cbo</i> FDH	1.7-fold increase of specific activity, values of K <sub>m</sub> formate and K <sub>m</sub> NAD increased from 6 mM and 45 mM to 14 mM and 74 mM, respectively
Role of loop between β-sheet and α-helix substrate specificity	Glu141Gln, Glu141Asn, <i>Par</i> FDH	Mutations Glu141Gln and Glu141Asn induced 5.5- and 4.3-fold increases in K <sub>m</sub> Formate values, 110- and 590-fold decreases in the kcat for reaction with formate and 9.5- and 85-fold increases in catalytic efficiency in reaction of glyoxylate reduction, respectively
Increase of operational stability Change of “essential” Cys, controlling <i>Pse</i> FDH operational stability. Cys255 is located above the plane of adenine moiety of NAD and occupies conservative position	Cys255Met, Cys255Ser, Cys255Ala, <i>Pse</i> FDH	Stable at least a month (200-fold increase in chemical stability), Decreased thermostability. K <sub>m</sub> <sup>NAD</sup> increased seven-fold for Met, three-fold for Ser and is the same as for WT for Ala; formate binding is unchanged for Ala and Ser and is three-fold decreased for Met.
Change of surface Cys354	Cys354Arg, Cys354Ser, Cys354Ala	Provided best thermal stability 1000-fold increased operational stability
Change of Cys145 near catalytically important Asn146	Cys145Ser	No changes in kinetic parameters and thermal stability
	Cys145Ala, <i>Pse</i> FDH	No changes in kinetic parameters and 10% decrease of thermal stability
Change of surface Cys354	Cys354Arg, Cys354Ser, Cys354Ala	Provided best thermal stability 1000-fold increased operational stability

**Table 1.1 (continued) : Important mutations in NAD<sup>+</sup>-dependent FDH [1].**

<b>Aim</b>	<b>Mutation/source</b>	<b>Result/conclusion</b>
Change of essential Cys in MycFDH (PseFDH and MycFDH differ by only two residues in positions 35 and 61)	Cys6Ser, Cys145/Ser, Cys255Ala/Ser/Val,	No data about kinetic properties and thermal stability.
	C146S/C256V, C6A/C146S/C256V, <i>MycFDH</i>	Increase of chemical stability was estimated by tolerance to inactivation by substrate ethyl 4-chloroacetoacetate and the yield of synthesis of ethyl (S)-4-chloro-3-hydroxybutanoate
Change of all available cysteines in <i>CboFDH</i>	Cys23(52)Ser, <i>CboFDH</i>	No change of kinetic parameters, increased chemical stability
	Cys262(288)Val, <i>CboFDH</i>	No change of kinetic parameters, diminished chemical stability
	Cys23Ser/Cys262Ala, <i>CboFDH</i>	No change of kinetic parameters, substantially decreased thermostability but operational stability under biotransformation conditions increased an order of magnitude
Increase of thermal stability Optimization of electrostatic interactions (effect of amino residues in positions 43 and 61 on thermal stability of bacterial FDH)	Glu61Gln, Glu61Pro	PseFDH and MycFDH differ by only two residues in positions 35 and 61
	Glu61Lys, <i>MycFDH</i>	Four- to six-fold lower thermostability of MycFDH is caused by electrostatic repulsion between Asp43 and Glu61 residues
	Lys61Arg, PseFDH	Mutation changed temperature dependence of thermal inactivation rate constant
Change of surface Cys354	Cys354Arg, Cys354Ser, Cys354Ala,	Provided best thermal stability 1000-fold increased operational stability
Change of Cys145 near catalytically important Asn146	Cys145Ser	No changes in kinetic parameters and thermal stability
	Cys145Ala, <i>PseFDH</i>	No changes in kinetic parameters and 10% decrease of thermal stability
Testing of role of Thr169 and Thr226 in stability of <i>C. methylica</i> FDH	Thr226Val	No change of kinetic parameters compared to wt- <i>CmeFDH</i> Decrease of enzyme stability by ~4 kcal/mol due to remove of hydrogen bond between this residues
	Thr169Val/Thr226Val, <i>CmeFDH</i>	

**Table 1.1 (continued) :** Important mutations in NAD<sup>+</sup>-dependent FDH [1].

<b>Aim</b>	<b>Mutation/source</b>	<b>Result/conclusion</b>
Improvement of thermal stability of CboFDH by directed evolution	Arg178Ser, <i>CboFDH</i>	Increase of thermal stability 3.1-fold and Tm 38 compared to SM
	Arg178Gly, <i>CboFDH</i>	Increase of thermal stability 2.2-fold and Tm 28
	Asp149Glu, Arg178Ser, <i>CboFDH</i>	Increase of thermal stability 6.7-fold and Tm 58, mutation Asp149Glu provides increase of thermal stability 2.15-fold
	Glu151Asp, Arg178Ser, <i>CboFDH</i>	Increase of thermal stability 27.6-fold and Tm 98, mutation Glu151Asp provides increase of thermal stability 9.0-fold
	Glu151Asp, Arg178Ser, Lys356Glu, <i>CboFDH</i>	Increase of thermal stability 18-fold and Tm 88, mutation Lys356Glu provides decrease of thermal stability 1.5-fold
	Glu151Asp, Arg178Ser, Lys306Arg, Lys356Glu, <i>CboFDH</i>	Increase of thermal stability 18-fold and Tm 88

### 1.2.2 Catalytic properties of NAD<sup>+</sup>-dependent formate dehydrogenase

The reaction that catalyzed by NAD<sup>+</sup>-dependent formate dehydrogenase is a suitable model for scientists who are trying to investigate the general mechanism of hydride ion (H<sup>-</sup>) transfer where direct transfer of H<sup>-</sup> ion from the substrate onto the C4-atom of the nicotinamide moiety of NAD<sup>+</sup> occurs without any acid-base catalysis steps [1].

NAD<sup>+</sup>-dependent formate dehydrogenases mainly follow Bi-Bi two-substrate order reaction mechanism. In this mechanism, NAD<sup>+</sup> is used as a first substrate and binding of NAD<sup>+</sup> increases the affinity of enzyme to secondary substrate for



approximately 3-fold. This reaction type is very common among significant portion of dehydrogenases [20].

Studies showed that kinetic properties of various NAD<sup>+</sup>-dependent formate dehydrogenase (from different origins) are very similar and ranging from 3 mM to 10 mM for formate and 35 μM to 90 μM for NAD<sup>+</sup>. Moreover, they can work in wide range of pH values from 6.0 to 9.0 and can keep their half of activity between 50°C - 60°C. However, it is quite possible that any mutation on NAD<sup>+</sup>-dependent formate dehydrogenase will lead to a dramatic change in its kinetic properties and cofactor specificities [13].

### **1.2.3 Structural properties of NAD<sup>+</sup>-dependent formate dehydrogenase**

NAD<sup>+</sup>-dependent formate dehydrogenases composed of two domains that are amino end (N-terminus) and carboxyl end (C-terminus) domains. It has reported that N-terminal domain has an important role in enzyme's activity.

In yeast and fungal NAD<sup>+</sup>-dependent formate dehydrogenases, there is no extra amino acid residue in N-terminal domains. In contrast, bacterial N-terminal domain of NAD<sup>+</sup>-dependent formate dehydrogenase is slightly longer and these additional amino acids contribute to its stability.

NAD<sup>+</sup>-dependent formate dehydrogenases has highly conserved amino acid sequence that have approximately 85% among different organisms. For *Candida* originated NAD<sup>+</sup>-dependent formate dehydrogenases, approximately around 46000 Dalton formed by 364 amino acids. Studies also showed that there is a big consensus on NAD<sup>+</sup>-dependent formate dehydrogenase's catalytically important residues. These residues are Pro77, Phe78, Ile102, Asn118, Ala/Gly171, Gly173, Gly176, Arg267, Gln287 and His310 for *cmFDH* and *cbFDH*.

The native form of *cmFDH* is a dimer and each subunit contains 364 residues folded into two distinct but structurally homologous domains. Each of these domains comprises a parallel β-sheet core that surrounded by α-helices. One domain functionally defined by coenzyme binding, the other by possessing the residues necessary for catalysis. The molecule dimerizes by two-fold symmetrical interactions between the coenzyme- binding domains while the catalytic domains are distal to the dimer interface [21-23]. Acid-base catalysis is an important feature of a number of NAD<sup>+</sup>-dependent dehydrogenases acting on 2-hydroxyacids [24, 25]. An invariant

pair of residues, histidine and a carboxylic acid, occupying conserved positions found in the active centers of a number of D- and L-specific dehydrogenases. They function as a composite acid-base catalyst facilitating proton transfer to and from the 2-hydroxylic group of the substrate [21, 22, 24, 25].

Crystal structures for both *Candida boidinii* formate dehydrogenase K47e mutant and *Candida boidinii* formate dehydrogenase C-Terminal Mutant are available in literature which are both have approximately 98% similarity with *Candida methylca* formate dehydrogenase. These mutant forms includes 12 histidine and 2 cysteine residues, shown in Figure 1.2, which allow enzyme to be partially interact with gold surfaces.

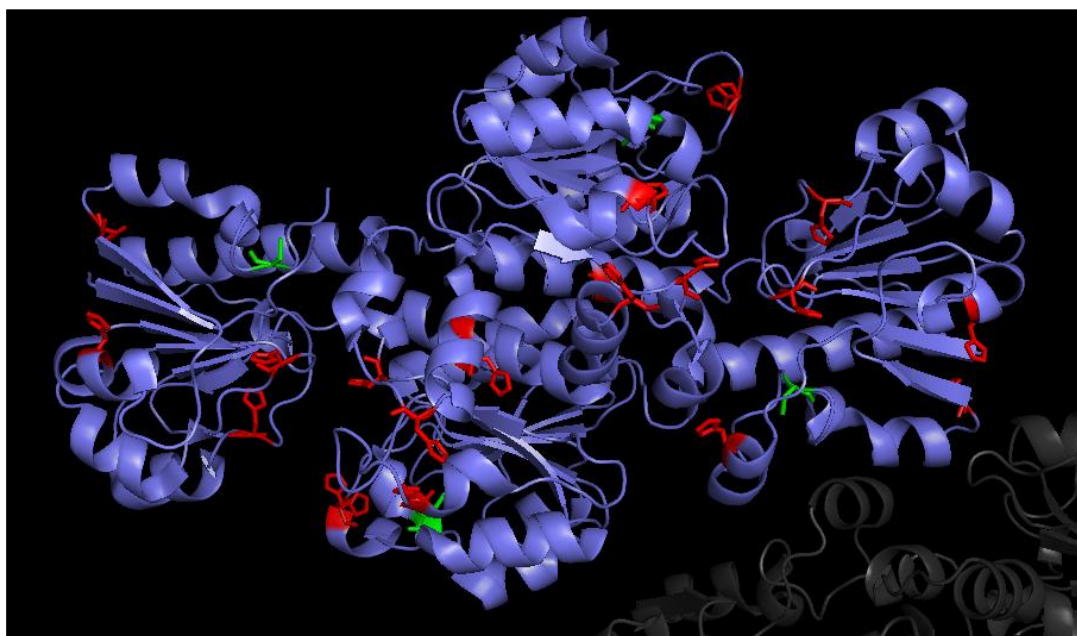


**Figure 1.2 :** Cartoon display of *cbFDH* (Histidine and cysteine residues are shown in red and green color, respectively.).

#### **1.2.4 Industrial applications of NAD<sup>+</sup>-dependent formate dehydrogenase**

After the prescriptions of the Food and Drug Administration about the optical purity of chiral compounds, the use of dehydrogenases in pharmaceutical era has sharply increased. Due to the dehydrogenases have great stereo-specificity in hydride ion transfer reaction, the use of these enzymes is very promising in order to produce optically active compounds with enough optical purity (more than 99.99%). However, the need for expensive coenzymes is a major drawback in this process. To overcome this problem by cofactor recycling, the use of NAD<sup>+</sup>-dependent formate dehydrogenases has been extensively increased in pharmaceutical industry [26].

Another biotechnological application of  $\text{NAD}^+$ -dependent formate dehydrogenases is the formate biosensors construction. Formate is an important fermentation product of many aerobic and anaerobic bacteria and abundant in the atmosphere, natural waters and sediments. However, conventional chromatographic methods are not simple enough to use for the quantitative determination of formate. With the development of highly sensitive formate biosensors, formate concentration can be found in a more faster manner with a linear detection range of 1–300 M, and the detection limit for formate is  $1.98 \times 10^{-7}$  M [1]. Some of examples about the reaction of FDH enzyme employed in industry can seen in Figure 1.3 below.

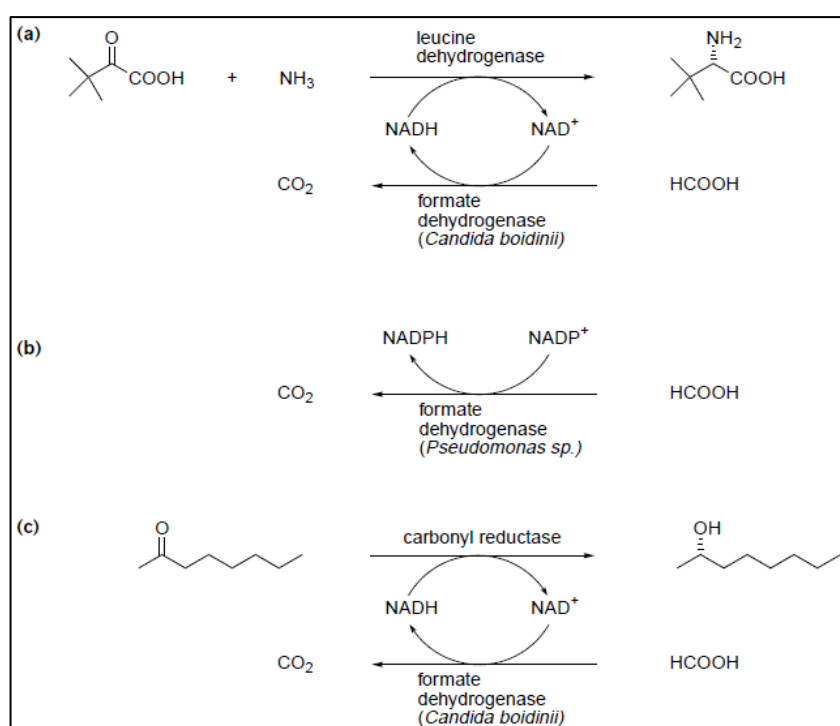


**Figure 1.3 :** Reaction of FDH employed in industry [26].

## 1.3 Protein Immobilisation Strategies

### 1.3.1 Physical adsorption

Intermolecular forces between proteins and the surface can be resulted to adsorb protein on surface by forming ionic bonds and hydrophobic or polar interactions.

The adsorption capacity of surface is mainly limited to size and distribution pattern of the protein. Self-Assembled Monolayer (SAM) construction on surface may help to increase loading capacity of the surface by forming specific hydrophobic or electrostatic low-energy interactions with proteins [27].

Intermolecular forces are enough to stabilize protein on surface to some degree but since the orientation of protein on surface is random and heterogeneous, it is generally impossible to utilize support surface area efficiently [27]. Moreover, since detergents and anti-ionic reagents disrupt ionic interactions between the surface and proteins, it is impossible to maintain these weak interactions in the presence of detergents. Polypropylene (PP) membranes modified with polyaniline (PANI), aspartic-modified dextrans and sulfate-modified dextrans are some examples in literature to this type of protein immobilisation method with SAM modified surface [28, 29].

### 1.3.2 Covalent immobilisation

Covalent immobilisation is the most frequently used method in literature. In this approach covalent bonds are irreversibly formed between functional groups of protein and support material. Functional groups exposed on surface are usually generated by chemical treatment and several pretreated surfaces are commercially available. Some of these groups are listed in Table 1.2.

Covalent immobilisation could be achieved with kinds of different procedures while some of them resulted with random orientation of protein and others are not.

**Table 1.2 :** Active sites for covalent attachment [27].

Side Groups	Amino Acids	Surfaces
-NH <sub>2</sub>	- Lys	carboxylic acid
	- Hydroxyl	active ester (NHS)
	- Lys	epoxy aldehyde
-SH	Cys	maleimide pyridyl disulfide vinyl sulfone
-COOH	Asp, Glu	amine
-OH	Ser, Thr	epoxy

### 1.3.2.1 Amine chemistry

The most commonly used attachment points are lysine's in this type of immobilisation approach due to their high probability to be present on the exterior part of the protein. However, their abundance in protein may sometimes results to multipoint attachment on support surface that restricts conformational flexibility of protein.

N-Hydroxysuccinimide (NHS) is the most commonly used agent for coupling with amine groups, forming stable amide bonds [30-34].

In this approach, proteins should dissolve in a low ionic- strength buffer and apply onto the surface. In this stage, NHS esters can react with  $\text{-NH}_2$  side groups of the proteins resulting with a strong amide bond that is shown in Figure 1.4.

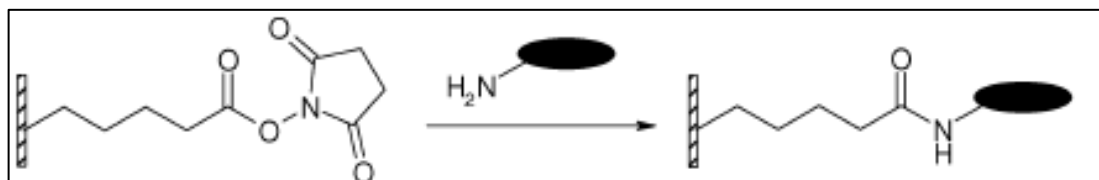


**Figure 1.4 :** Amine chemistry on NHS-derivatized surface [27].

In this strategy, pH, concentration, ionic strength, and reaction time are significant parameters that should precisely optimized.

In 1997, catalase enzyme successfully immobilized and the effects of the accessibility of terminal carboxylated groups of SAM on reaction with NHS were criticized [33].

Another strategy to utilize amine groups on proteins with the purpose of covalent attachment is to generate aldehyde groups via surface modification shown in Figure 1.5 below [35-38].

MacBeath and Schreiber constructed the first protein microarray in 2000, by stably immobilizing proteins onto aldehyde-derivatized glass slides via their  $\text{NH}_2$  groups [38].

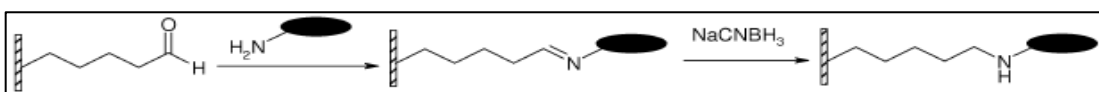


**Figure 1.5 :** Aldehyde-derivatized surfaces [27].

### 1.3.2.2 Thiol chemistry

Cysteine amino acid has the ability to form internal disulfide bonds with its unique thiol group. In this type of strategy, random immobilization is less likely to occur due to the less abundance of cysteine residues in proteins.

To create disulfide bond between thiol group of cysteine residues and surface, three different surface functionalization methods has developed.

First one is the maleimide derivatization strategy, that is shown in Figure 1.6, in which double bond of maleimide group undergoes an addition reaction with thiol groups to form stable thio-ether bonds at specific pH range of 6.5-7.5 [39-41].

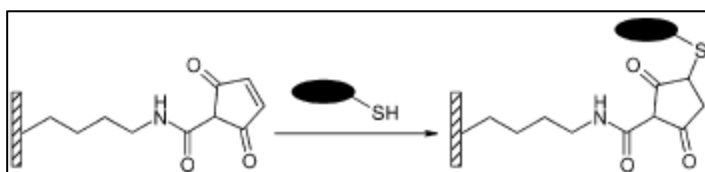


**Figure 1.6 :** Maleimide-derivatized thiol chemistry on surfaces [27].

In disulfide-derivatized thiol chemistry approach that is shown in Figure 1.7, disulfide reagents participate in disulfide exchange reactions with group to form a new mixed disulfide. Pyridyl disulfides are the most commonly used reagents.

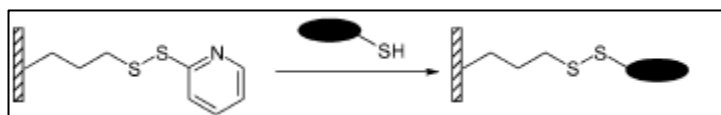


**Figure 1.7 :** Disulfide-derivatized thiol chemistry on surfaces [27].

In Michael addition reaction, the vinyl sulfone groups react with -SH groups by a conjugate addition reaction. The main advantage of this reaction is its ability to generate bond formation under mild and physiological conditions. [42] In this reaction, electrostatic environment of the thiol groups are very important due to the fact that deprotonated thiol groups are more reactive than thiol groups species in the Michael addition reaction, shown in Figure 1.8 below [43].

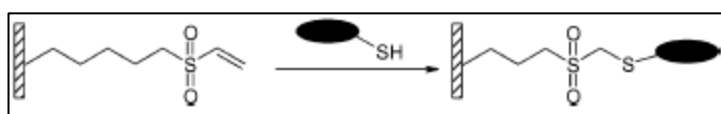


**Figure 1.8 :** Vinyl sulfone-derivatized thiol chemistry on surfaces [27].

### 1.3.2.3 Carboxyl chemistry

Immobilization of proteins via their carboxyl groups shown in Figure 1.9 is another effective strategy in literature. Since aspartic and glutamic acid usually located in the outer parts of the protein, immobilisation could easily achieve without a significant activity loss.

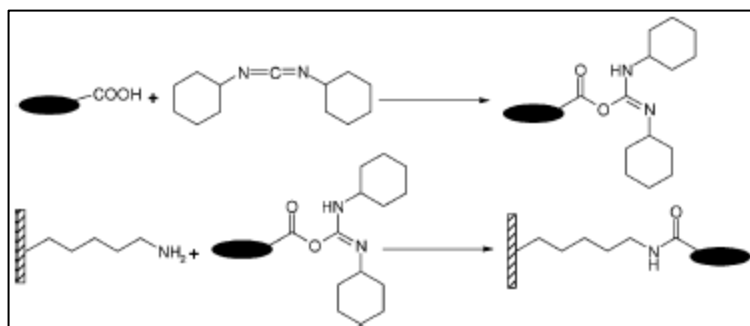


**Figure 1.9 :** Carboxyl chemistry using carbodiimide activation [27].

In this strategy, carboxyl groups in proteins should be activated via carbodiimide (CDI) treatment. In 1993, Fernandez and his colleagues achieved to immobilize  $\beta$ -galactosidase from *Aspergillus oryzae* onto a solid support surface [32, 44].

### 1.3.2.4 Photoactive chemistry

Photo immobilization is based on the activation of photosensitive reagents by the incident light of an appropriate wavelength and their ability to form covalent bonds between these photo-generated intermediates and the biomolecules.

In this strategy, specific heterobifunctional photolinkers having one photoreactive group and one chemical reactive group are utilized. These heterobifunctional photolinker molecules have the ability to react with a solid support surface via irradiation and to the protein via a chemical process or vice versa. In 1993, Collioud et al. achieved to immobilize peptides onto glass and polystyrene surfaces by using the heterobifunctional crosslinker reagent *N*-(*m*-(3-(trifluoromethyl)-diazirin-3-yl)phenyl)-4-maleimido butyramide (MAD) [45]. Photo immobilization technique offers several advantages which are briefly mentioned and discussed in several different review papers [46, 47]. First of all, the photoreaction is a single-step process and does not need functionalization of the target molecules. Hence, it can be utilized for immobilizing biomolecules lacking active functional groups in a fast and efficient manner. Secondly, the reaction takes place in physiological conditions

which is very important working with biomolecules. The most commonly used photoreagents are arylazides, diazirines, benzophenones, and nitrobenziles which are biologically compatible [27].

### 1.3.2.5 Peptide ligation

The main significance of this approach is its strictly controlled uniform and well oriented protein immobilization. The chemo selective capture needs two proximally placed nucleophile or electrophile groups at both ends of the protein that are compatible to each other. These compatible nucleophile and electrophile pair brings the N- and C-termini into a close proximity to permit an intramolecular acyl transfer reaction forming an amide bond. Cysteine, serine, histidine, and threonine have been found to be the most suitable amino acids due to the fact that they contain weak-base nucleophiles such as thiol, amine, or hydroxyl groups. For the C-terminus, an ester or a thioester is required. The ligation between N-terminal cysteine and ester glycoaldehyde residue on support surface leads to the formation of a thiazolidine ring, followed by an acyl migration to form a proline mimic [30, 37, 48, 49]. The Figure 1.10 below schematizes the peptide ligation reaction.

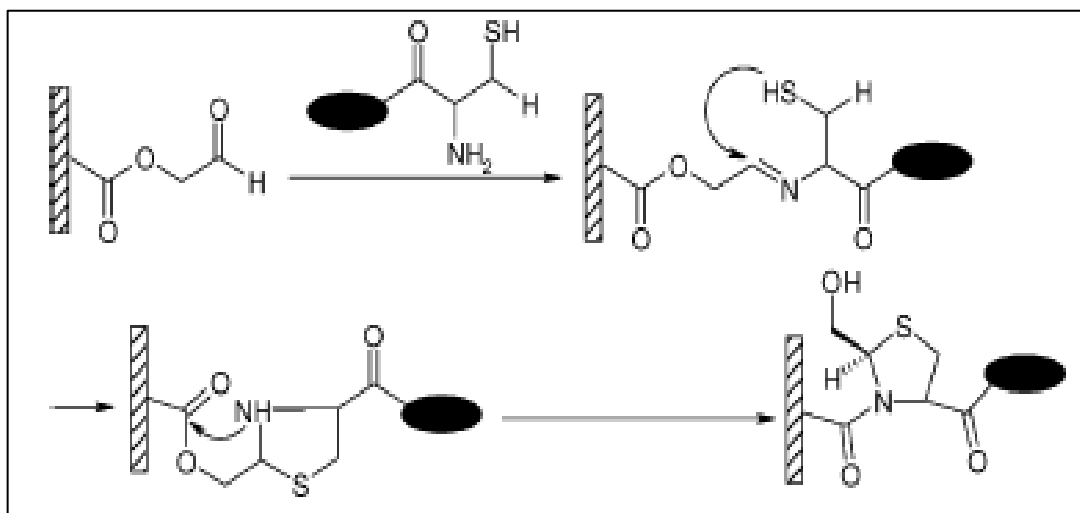


**Figure 1.10** : Peptide ligation [27].

### 1.3.3 Affinity

Affinity immobilization reactions carried out in mild conditions and offer well oriented immobilization. Moreover, it is possible to detach proteins from support surface via affinity immobilization which make repeated use of the same possible.



### 1.3.3.1 Avidin-biotin system

The use of avidin-biotin technology as an immobilization strategy has been briefly described in literature by several review papers [27].

This strategy is mainly based on the one of the strongest non covalent bonds where the dissociation constant ( $K_d$ ) is equal to  $10^{15} \text{ M}^{-1}$ . The strength of this bond leads to a very specific interaction resulted with uniformly oriented protein immobilization [32].

Avidin is a soluble, tetrameric glycoprotein that is very stable over wide range of pH and temperature. One avidin molecule can bind up to four molecules of biotin by a very rapid bond formation where the reaction is independent and not affected from pH, temperature, organic solvents, enzymatic proteolysis, and other denaturing agents. Streptavidin is a closely related tetrameric protein. Though it differs from avidin in terms of molecular weight, amino acid composition, and pI value, it has very similar affinity to biotin that makes it suitable to utilize in avidin-biotin immobilization strategy [27].

Biotin (or vitamin H) is a common naturally occurring vitamin that is found in all living cells. Since only its bicyclic ring is required to form interaction with avidin; its carboxyl group on the valeric acid side chain can be modified in order to generate active biotin molecules known as biotinylation reagents that are used for generating biotinylated proteins. With this approach, there are several biotinylation reagents have been developed. The NHS ester of biotin is the most commonly used biotinylation reagent which mainly used in order to target amine groups of proteins and biotin hydrazide which commonly used in order to target carbohydrates and carboxyl groups of proteins [27].

A typical biotin/avidin/biotin multilayer is composed by biotin directly immobilized and avidin creating a secondary layer for binding biotinylated molecules that is seen Figure 1.11 below.

This approach is generally preferred due to the higher organization obtained in comparison to that of the direct immobilization of avidin. Moreover, due to its small size, conjugation of biotin molecule to proteins does not affect their conformation, size, or functionality [27].

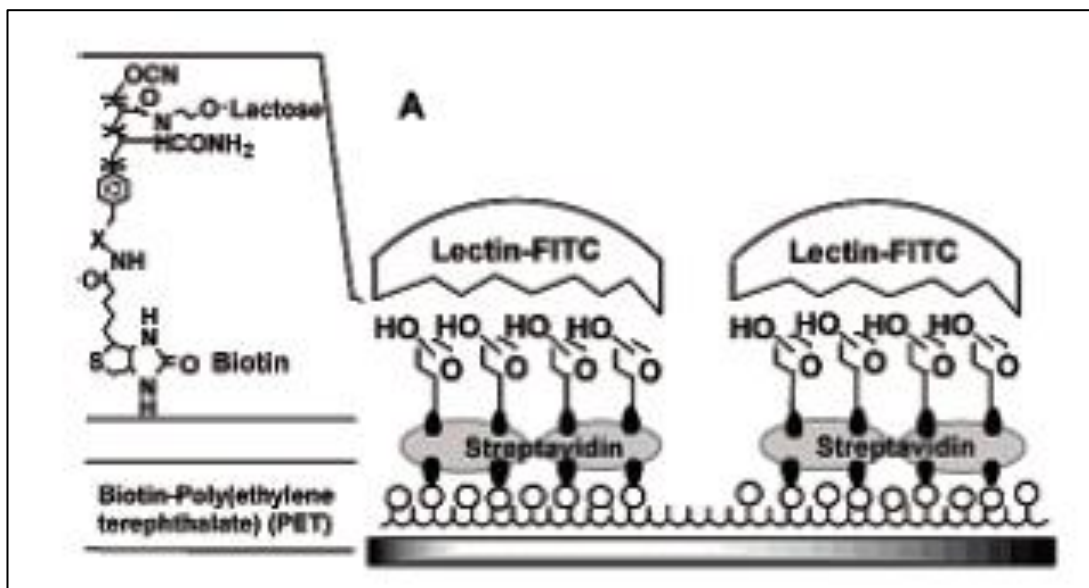


**Figure 1.11** : Glycopolymer-derivatized surface via a biotin-streptavidin layer [27].

### 1.3.3.2 Polyhistidine-tag system

Polyhistidine-tag (His-tag) is the one of the most commonly used tag system with its several advantages such as small size, compatibility with organic solvents, low immunogenicity, and effective purification under native and denaturing conditions. Proteins with six histidine residues (6xHis) at their C- or N-terminus can be stabilized via a nickel chelated complex, like Nickel-Nitrilotriacetic Acid (Ni-NTA).

In Histidine-tag immobilization system, Ni-NTA is covalently bound to the surface in order to functionalize the surface of support. When 6xHis-tagged proteins applied onto surface modified via Ni-NTA, the specific chelating interaction between NTA and imidazole rings of 6xHis-tagged protein occurred, shown in Figure 1.12.

In comparison to covalent attachment, the interaction between the Ni-NTA and 6xHis are quite low with  $K_d$  value. However, this interaction is highly specific and entirely reversible upon addition of a competitive ligand, such as histidine or imidazole.

Immobilization via Polyhistidine-Tag and Ni-NTA serves several advantages. The reusability of this system, irreversible binding of tagged proteins on support material and well oriented binding are some of the important advantages of this system. Moreover, His tag system is commercially available for a large number of functional proteins [50-54].

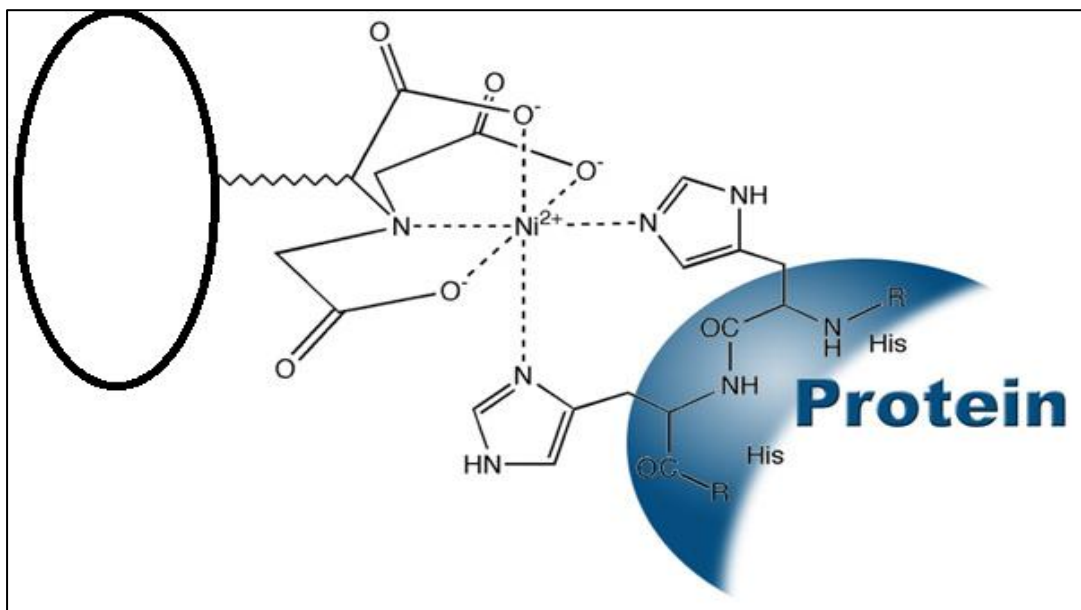


**Figure 1.12 :** Binding of His-tagged proteins on a Ni-NTA surface [50].

### 1.3.3.3 Protein A/ protein G-mediated immobilisation

The strategy of Protein A/Protein G-mediated Immobilization is based on the interaction between the Fc constant region of IgG molecules and its specific antigen molecule shown in Figure 1.13 below.

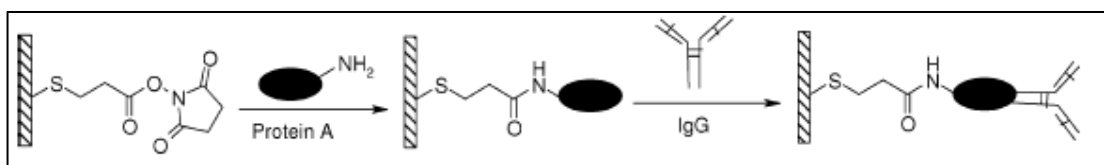


**Figure 1.13 :** Antibody immobilization using a layer-by-layer architecture [27].

There are several reviews about this strategy and applications in immunoassays and affinity chromatography are readily available in literature [55, 56]. In this strategy, it is ensured that the binding site of the antibody that is located on the Fab variable region always remains well accessible for binding with the antigen.

In 2003, the use of protein A with the purpose of immobilizing human IgG on a silicon surface was proposed by Wang et al [55].

One of the most important drawbacks of the protein A-mediated immobilization is the lack of control on the orientation of protein A. To overcome this problem, approaches were presented. In 2003, Johnson et al., proposed the addition of 6xHis tag to the C-terminus of protein A to obtain oriented immobilization [55]. Moreover,

in 2005, Lee et al. overcome same problem via fabricating an ordered layer-by-layer architecture, with a self-assembled *N*-succinimidyl-3-(2-pyridyldithio) propionate (SPDP) layer reacting with the primary amine of protein A.

### 1.3.4 Protein immobilisation strategies

In protein immobilization, the physical and chemical properties of support materials such as their nanostructure, hydrophilic or hydrophobic properties, and charges are very important. Several nanomaterials have been developed and extensively employed in literature with their exceptional properties in immobilization systems. Table 1.3 summarizes some of the widely used approaches below.

**Table 1.3 :** Application of protein immobilisation [57].

Application	Enzyme	Reactions	Carrier	
			Attachment	Method
Biosensor	Glucose oxidase	Glucose oxidation	Silica	Nanoporous matrix
		Glucose oxidation	Zinc oxide	Nanorod
		Glucose oxidation	Indium tin oxide	Layer-by-layer dendrimer nanoparticle
		Glucose oxidation	Gold/polycarbonate composite	Porous nanoparticle
Biosensor	Horseradish peroxidase	H <sub>2</sub> O <sub>2</sub> oxidation	Gold	Membrane Nanoparticle
		H <sub>2</sub> O <sub>2</sub> oxidation	Cysteamine-capped gold	Nanoparticle
		H <sub>2</sub> O <sub>2</sub> oxidation	Copper	Nanoporous particle
Food industry	$\alpha$ -Amylase Diastase Lactase Lipase	Starch hydrolysis	Halloysite	Nanotube
		Starch hydrolysis	Octadecanoic acid/silica composite	Porous nanoparticle
		Lactose hydrolysis	Gold	Nanoparticle
		Olive oil hydrolysis	Silica	Nanosphere
Pharmaceutical approach	L-lactate dehydrogenase	Conversion of 2-oxo acids into (S)-2-hydroxy acids	Silica coated magnetic cluster	Nanoparticle
	Penicillin G acylase	Penicillin G hydrolysis	Silica	Nanoporous material
		Penicillin G hydrolysis	Silica	Porous hollow nanotube
Environmental technology	Lignin peroxidase	Penicillin G hydrolysis	Silica	Mesoporous foam
		Dye decolorization	Gold	Nanoporous particle

**Table 1.3 (continued) : Application of protein immobilisation [57].**

Application	Enzyme	Reactions	Carrier	
			Attachment	Method
Bioenergy (Bio fuel cell)	Glutamate dehydrogenase	Glucose oxidation	Gold	Porous electrode
Bioenergy (Biorefinery)	Laccase	Lignin oxidation	Zinc tetraaminophthalocyanine- iron oxide (Fe <sub>3</sub> O <sub>4</sub> )	Nanoparticle
Environmental technology	Lignin peroxidase	Dye decolorization	Gold	Nanoporous particle

#### 1.3.4.1 Gold nanoparticles

Gold nanoparticles (AuNPs) have high affinity for biomolecules either with or without linkers. Gold surface could modify easily via sulfur-containing compounds like alkane thiols and ditiocarbamates. Self-assembled monolayers (SAMs) of alkane thiols on the surface of gold containing a functional terminal group lead to interact with additional molecules such as enzymes by via covalent conjugation, supramolecular association, physical adsorption and electrostatic interactions [57-61]. Moreover, it has been also suggested that immobilization onto gold surface contribute enzyme's colloidal stability, which leads to significantly enhanced catalytic activity, even though there is no modification has been carried out [58].

Nanoporous gold electrodes serves increased surface area that makes them very convenient support material in enzyme immobilization with their high loading capacities.

Nanosphere shape gold nanoparticles are also widely employed structures among gold nanoparticles [57].

#### 1.3.4.2 Carbon nanotubes

Carbon nanotubes (CNTs) have started to employ in biosensor studies as an electrode modifying materials due to their high electrocatalytic features. They have also employed in enzyme immobilization studies because they can broadly functionalized and have good dispersion in solution in comparison other nanomaterials [57, 62].

In 2010, Lee et al., successfully achieved to improve electrical properties of an anode surface on an enzyme- based biofuel cell via immobilization of glucose oxidase on single walled nanotubes. In another study in 2010, it was reported that sulfonated polyaniline network was formed on multi-walled carbon nanotubes (MWNTs) and

glucose oxidase enzyme was successfully immobilized onto this polyaniline matrix in order to fabricate the biosensor [57, 62].

### 1.3.4.3 Magnetic nanoparticles

Laborious separation process from solution may sometimes be a significant drawback on the use of nanomaterial in enzyme immobilization. Magnetic supports such as magnetite nanoparticles allow easy enzyme recovery from the medium under the magnetic force without needing expensive liquid chromatography systems, centrifuges, filters or other equipment.

These magnetite nanoparticles are highly hydrophobic in aqueous solution and thus generally cause aggregation. To overcome this problem, the surface of magnetite nanoparticles coated with silica. Silica coated magnetic nanoparticle with specific surface modification like containing amino, aldehyde and alkyl chain groups are now commercially available [57].

### 1.3.4.4 Porous silica structures

Due to the low enzyme loading capacity of nonporous silica nanoparticles, porous nanoparticles have developed with expanded surface area. Among different types of porous silica particles, mesoporous silica nanoparticles the most attractive one with their high surface area, controllable pore diameter, and uniform pore size distributions [63]. The schematic view of fabrication of mesoporous silica nanoparticles is shown in Figure 1.14 below.

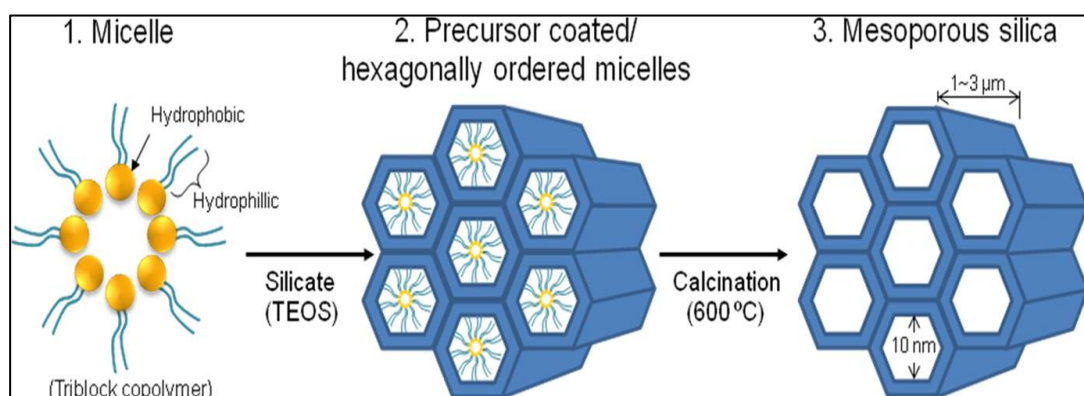


**Figure 1.14 :** Schematic fabrication of mesoporous silica nanoparticles [63].

Currently, various types of mesoporous silicas have synthesized such as MCM-41, SBA-15 and mesocellular foam (MCM) [57, 63].

## **1.4 Genetically Engineered Peptides for Inorganics (GEPI)**

Over the last decade, genetically engineered peptides for inorganic solids (GEPIs) have emerged, taking advantage of molecular biomimetics where different disciplines such as materials science and molecular biology utilized to understand the interactions between materials and biomolecules by taking lessons from the nature. Recent studies pioneered by Sarikaya and his co-workers have demonstrated that inorganic-binding peptides have great potential for various applications in different areas in conjunction with nanotechnology such as nanobiotechnology, medicine, nanoelectronics. Following successful isolation and characterization of these peptides, they started to used as assembler, linkers, and synthesizers in proof-of-principle implementations. To be able to demonstrate the development towards novel functional materials, this section includes isolation and characterization of GEPIs as well as their potential applications [64-71].

### **1.4.1 Combinatorial methods for selecting first generation GEPI's**

Advances in recombinant DNA technologies, combinatorial selection technology tools, emerged two decades ago, have started to utilize in studies about the characterization of antibody-receptor, protein- or peptide ligand interactions. Among kinds of combinatorial selection tools, bacterial cell surface display and phage display are two of the mostly employed techniques in literature.

In 1992, the first peptide selection via combinatorial selection tools was made by Brown et al., with the aim of finding a peptide sequence that specifically binds to  $\text{Fe}_2\text{O}_3$ . Following to this, our group and others have achieved to identify various peptide sequences that are specifically and selectively binds to the surfaces such as noble metals including Au, Ag, and Pt, oxides including  $\text{SiO}_2$ , ZnO,  $\text{Cu}_2\text{O}$ ,  $\text{TiO}_2$  minerals including hydroxyapatite, calcite, sapphire and semiconductors including GaN, ZnS, and CdS via using combinatorial selection tools.

Both of these bacterial cell surface display and phage display techniques based on displaying specifically inserted random sequences into the bacteria or phage genome and expressing them to produce a huge library. With this aim, in bacterial cell surface display method various outer membrane proteins of cell such as lipoproteins, fimbriae and flagellar proteins, Figure 1.15, have been widely utilized to display the randomized peptide library on surface.

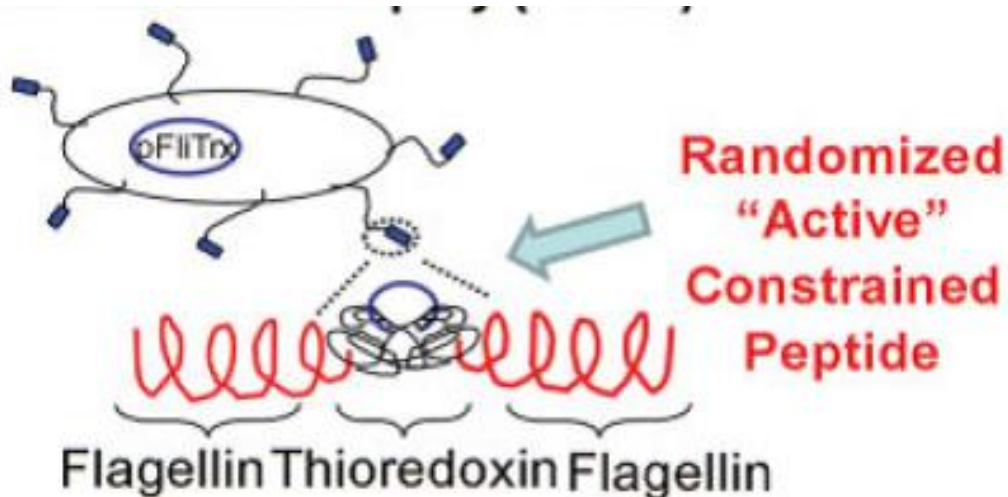


**Figure 1.15 :** Insertion site of the random peptide library in cell surface display system [64].

In phage display method, however, only the major and minor coat proteins of M13 bacteriophage can be used.

In vitro selection of GEPIs are carried out by a biopanning step in which the library of phage or cell clones, displaying a vast population of randomized peptides on their surfaces, is exposed to inorganic targets. Next, the unbound clones are washed away by a standard washing step and the remaining bound ones are eluted via physical or chemical methods such as treatment with buffer containing certain amounts of detergent and probe sonication. To obtain the best clones with the highest affinity, this biopanning process is usually repeated 3-5 times with increased stringency of wash buffers. In the final step, individual clones showing the highest affinities are isolated and their displayed peptide sequences are identified by DNA sequence analysis. Figure 1.16 gives a brief description of both cell surface and phage display methods.

After DNA analysis, clones are identified by a protocol developed by Sarikaya's group. According to this protocol, first each clone is applied to an inorganic surface and bound clones are labeled with M13-antibody-FITC conjugate or DNA dye in case of being phage or cell. After that, bound clones are counted in order to calculate the surface coverage of these clones semi-quantitatively via fluorescence microscopy (FM) or ELISA, in case of being cell surface or phage, to assess the affinity levels of individual clones. According to the surface coverage percentages of each clone, they are identified as weak or strong binders. These first-generation peptides can be used either directly or after additional engineering steps to further develop their affinity kinetics.



by computational biomimetics approaches to more functionally specific peptides [72].

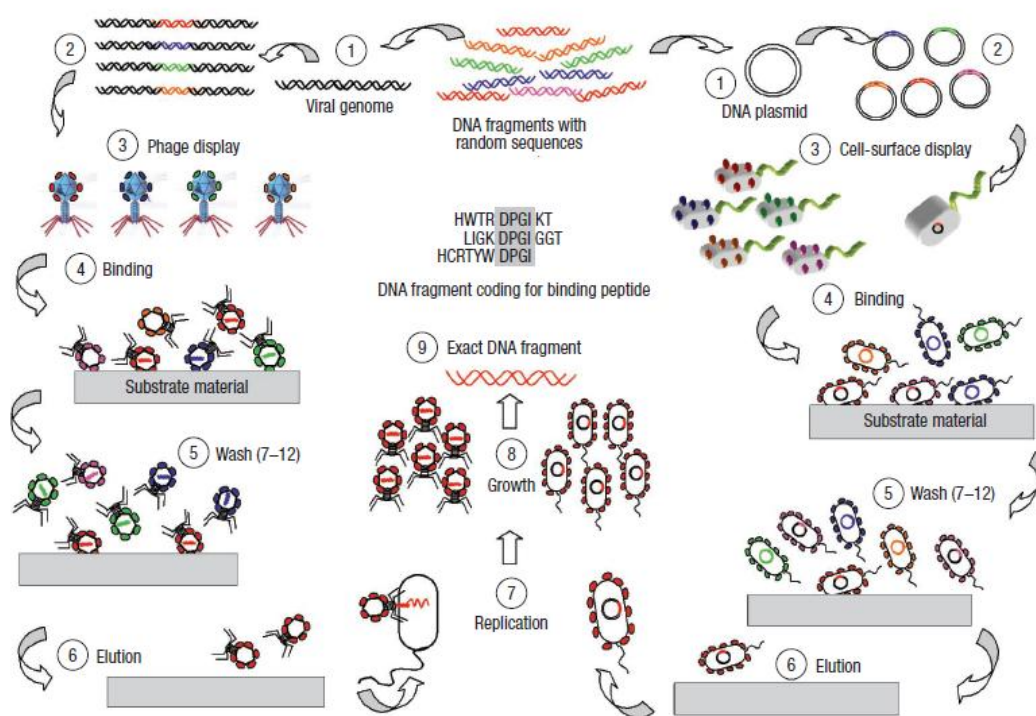


**Figure 1.16** : Schematic view of cell surface display and phage display methods [72].

#### 1.4.2 Computational biomimetics for further characterization of GEPIs

Size of the library that is constructed to select peptides for inorganic materials may not be enough to cover all possibilities to reach the best sequence through directed evolution [66]. Therefore, experimentally selected peptides are further studied in order to improve their binding abilities and material-specificities via computational biomimetic approaches.

The interaction between proteins and solid materials in nature has been studied for decades. These studies showed that the different proteins that bind to similar solid surfaces shows great sequence similarity to each other. Based on these findings, Sarikaya and his co-workers hypothesized that one surface may need sequence similarity to a certain level among peptides that are selected for a same material.

Starting with this theory, with the aim of designing new peptides with enhanced affinities Sarikaya and his co-workers developed a unique method that combines

different sequence alignment techniques resulting in material specific scoring matrices, seen in Figure 1.17 [65].

With this method first of all, sequence selection is performed prior to the characterization studies of inorganic binding peptides for specific materials. Consequently, peptides classified according to their material-binding affinities as strong, moderate or weak binder. In the next step, sequence alignment and standard scoring matrices applied to the previously characterized sequences with the aim of generating novel material specific sequence scoring matrix that would account for the specific sequence patterns responsible for binding as opposed to sequence patterns found in weak binding group.

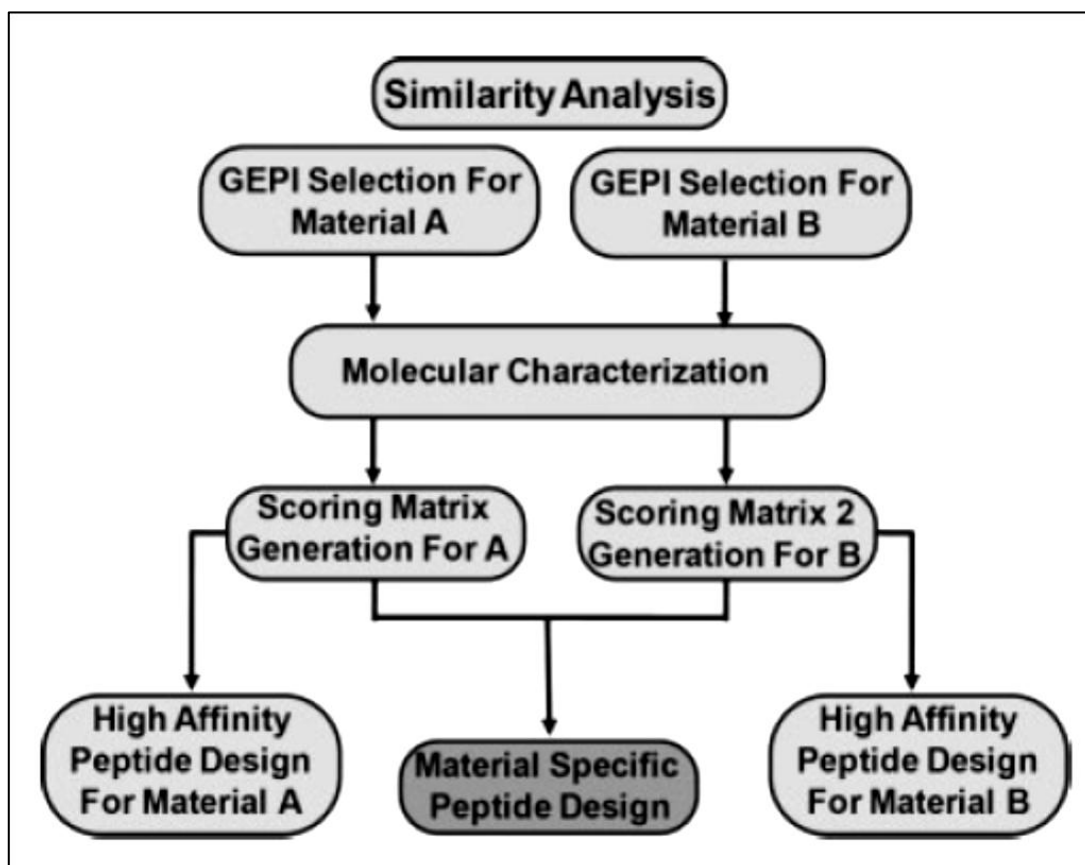


**Figure 1.17 :** Knowledge based approach in generating next generation of peptides with superior binding properties [64].

### 1.4.3 GEPI as a bifunctional immobilisation tool

Combinatorially selected inorganic binding peptides (GEPI) have various practical applications in nanoscience and nanotechnology with their exceptional binding and self-assembly characteristics onto the inorganic solid surfaces. Their exceptionally

high binding affinity and selectivity capabilities make them very useful and convenient bifunctional molecules that can be a novel alternative method to conventional immobilization techniques on which scientist have been studying for years in order to deal with certain limitations.

In the previous immobilisation studies in literature, biomolecules are usually stabilized via forming covalent bonds with either bare surface or SAMs that are previously constructed or each other. Physical adsorption of proteins via electrostatic interactions with surface is also widely employed technique, albeit the interaction with the solid surface is very weak. Random orientation, protein inactivation, lack of ordered assembly and low durability are the some of the common drawbacks of these above mentioned conventional methods.

Therefore, to overcome all of these certain limitations in protein immobilization more robust coupling methods and material specific, biomolecule-friendly linkers are needed [70]. At this point, combinatorially selected 18-aa (CGPWALRRSIRRQSYGPC) cyclic Gold Binding Peptide (c-AuBP2) provide a good alternative as a bifunctional molecule with its unique binding characteristics ( $K_{eq}=13,50 \times 10^6 \text{ M}^{-1}$  and  $\Delta G_{ads} = -9,7 \text{ kcal/mol}$ ) on gold surface [67, 73].

### **1.5 Surface Plasmon Resonance (SPR) Spectroscopy**

Surface Plasmon Resonance Spectroscopy is a highly sensitive spectroscopic characterization method for molecular interactions. The mechanism of SPR sensing is the resonance of surface plasmon which are surface free electrons of metal [74] that is usually gold. Being a spectroscopic method, SPR harnesses surface electrons of gold that are excited by a light source which transfers energy to the electrons resulting a wave like oscillation of electrons [75]. This medium on the surface is very sensitive to the changes occur within the environment and directly related with the optical characteristics of the systems [74]. Thus SPR uses the refractive index change of the system which can be correlated with deposited mass on the metal surface by mathematical models [76]. Hence a small change on the metal surface can be detected precisely and used for quantitative measurement of the target molecules in a design for a real time process. In fact SPR spectroscopy is used not only for surface molecular interactions but also can be applied to molecule-molecule interactions. Protein or any other biomolecules can immobilized on the gold surface of SPR

spectroscopy system to measure the interactions of another (bio)molecule(s). The advantage of this system lies on the ability to provide both qualitative and quantitative results about association and dissociation of the molecules [74]. In addition it is possible to obtain information about thermodynamic properties of the interaction. This information is especially important on the characteristics of the binding event that is under examination while studying protein-surface or protein-protein interactions. Gold binding peptide (GBP) in this context is a very advantageous biomolecule to be used and characterized by SPR spectroscopy. Using GBP it is possible to immobilize any biomolecule directly to the gold surface of SPR spectroscopy systems [77]. Genetically fused GBP to the target molecule opens up a new approach to bind biomolecules to the metal surface for further analysis of binding and dissociating mechanisms. GBP is superior when compared with conventional immobilization techniques since these chemical modifications involve mostly organic molecules that have high affinity to gold on one side and an attractive chemical group to target biomolecule on the other side [78]. The disadvantage of these synthetic molecules is the unspecific binding of target molecules to the coated surface. Unspecific binding could lead to occupy active sites of proteins specifically enzymes which decreases their activity [77]. On the contrary, GBP could be fused to either N or C terminus of target molecules which results in high self-assembly and stable enzymatic activity [77]. In conclusion SPR spectroscopy is an appropriate analysis technique for quantitative and qualitative protein interaction especially when used with GBP fused biomolecules with its enhanced gold binding capability.

## 2. MATERIALS AND METHODS

### 2.1 Materials

Materials are listed in Appendix A.

#### 2.1.1 Laboratory equipments

Laboratory equipments are listed in Appendix B.

### 2.2 Methods

#### 2.2.1 AuBP2 selection

AuBP2 peptide was combinatorially selected and characterized by our group in 2008. The selection and characterization study was briefly described in results section.

#### 2.2.2 AuBP2-FDH fusion protein construction

AuBP2-FDH fusion protein was constructed by the addition of and *cyclic*-AuBP2 (CGPWALRRSIRRQSYGPC) sequences to the N terminal of *cm*FDH (*Candida methylca* formate dehydrogenase). With this aim, wild type FDH (wtFDH) sequence were obtained into the pQE2 His-tag expression vector (Qiagen, USA) and AuBP2 sequence is added onto the N-terminal of the wt-FDH by using two step PCR with four different forward and one reverse primer sequences shown in Table 2.1 below.

In the first step of PCR primers, named with Forward Primer 1 and Reverse primer, used the under the specific PCR conditions shown in right side of Table 2.2. In this PCR amplification was done in 15 cycles.

**Table 2.1** : Primer sequences used in fusion protein construction.

Primer Name	DNA sequence
Forward Primer 1	5'AGATCCATCAGGAGACAGTCCTACGGTCCTTG CGGTGGTGGTTCCATGAAGATCGTTTTAGTC 3'

**Table 2.1 (continued) : Primer sequences used in fusion protein construction.**

Primer Name	DNA sequence
Forward Primer 1 short	5'AGATCCATCAGGAGACAG 3'
Forward Primer 2	5'TAGAGAGCTCAATGCGGCCCTTGGGCCCTGAG GAGATCCATCAGGAGACAG 3'
Forward Primer 2 short	5'TAGAGAGCTCAATGCGGCCCT 3'
Reverse Primer	5'TTCCCTGCAGTTATTTCTTATCGTGTTTACC 3'

**Table 2.2 : PCR conditions (1<sup>st</sup> Step) used in fusion protein construction.**

Reagents	Volume (μL)	Reaction Conditions
Expand High FidelityPLUS PCR System 5X Buffer	4	94°C 2 min
dNTP (10 uM)	0.3	94°C 20 sec
Primer 1 (10 uM)	1	50°C 30 sec
Template	1	72°C 4 min
Enzyme Mix	0.2	
dH2O	13.5	72°C 7 min
Total Volume	20.0	

The resulting amplified fragments used as a template of second step PCR according to the conditions shown in Table 2.3. In this PCR, primers named with Forward Primer 1 short and Reverse Primer were used and the amplification continued for 30 cycles.

After that both of the first and second step PCR's repeated by second primers to obtain full-length AuBP2 sequence with same conditions in Table 2.2 and 2.3. After that whole PCR products were visualized and verified by 1% agarose gel electrophoresis to check integrity and yield. All of the PCR reaction loaded into the gel to purify the PCR product.

After electrophoresis, corresponding band was cut by sterile, sharp scalpel and transferred to a clean 2 mL tube. Extraction performed by QIAGEN – QIAquick Gel

Extraction Kit (Qiagen, USA), according to the gel extraction procedure described in kit manual. In this procedure, first of all cutted gel slice was weighted and 3 volumes of commercial Buffer QG added onto gel. Then the mixture incubated at 50 °C for 10 minutes by mixing it in every 3 minutes in order to dissolve completely. After dissolving the gel slice completely, 1 gel volume of isopropanol was added to the sample and mixed. In the next step, the complete sample transferred to commercial MinElute column and centrifuged at 13000 rpm for 1 minute. After discarding the flow through, 500 µL of QG buffer added to the column and centrifuged again at 13000 rpm for 1 minute. Then the supernatant discarded again and sample washed with 750 µL of commercial PE buffer. Finally, the sample eluted by 10 µL of EB Buffer containing 10 mM Tris-Cl, pH 8.5, and the fragment obtained.

**Table 2.3 :** PCR conditions (2<sup>nd</sup> Step) used in fusion protein construction.

Reagents	Volume (µL)	Reaction Conditions
Expand High FidelityPLUS PCR System 5X Buffer	4	94°C 2 min
dNTP (10 uM)	0.3	94°C 20 sec
Primer 1 short & reverse (10 uM)	1	50°C 30 sec
Template	1	72°C 4 min
Enzyme Mix	0.2	
dH2O	13.5	72°C 7 min
1St Step PCR	20.0	

Next, isolated AuBP2-FDH fragment cloned directly into the pQE2 expression vector without any subsequent TA cloning steps. With this purpose, at first both constructed fragment and empty pQE2 plasmid vector was digested with PstI and SacI restriction enzymes and reaction clean-up process was performed to total digestion reaction by using Qiagen MinElute Reaction Cleanup kit (Qiagen, USA) according to the procedure described in kit manual. In this procedure, first 300 µL of Buffer ERC added onto the enzymatic reaction and mixed. Then the mixture applied to the sample column and centrifuged for 1 minute to let sample bind to the column. After discarding the flow-through the sample washed with commercial Buffer PE twice and eluted with 10 µL of Buffer EB containing 10 mM Tris·Cl, pH 8.5.

Concentrations of the constructed fragment and empty pQE2 plasmid determined by 1% agarose gel analysis again and ligation reaction was set up with Roche Rapid DNA Ligation kit (Roche, Switzerland) according to the DNA Ligation procedure. With this aim first the vector DNA (pQE2) and purified DNA fragment were dissolved in 1x DNA Dilution Buffer to a final volume of 10  $\mu$ L and 10  $\mu$ L of T4 DNA Ligation Buffer added to the reaction to final volume 20  $\mu$ L. Finally, 1  $\mu$ L of T4 DNA Ligase added and reaction incubated at 25°C for 10 minutes.

For transformation, 7  $\mu$ L of ligation reaction added into 50  $\mu$ L of E.coli DH5 $\alpha$ -T1 chemically competent cell (Invitrogen) and the solution was incubated on ice approximately 30 minutes. Then heat shock was performed at 42°C during 30 seconds and cells were incubated on ice again during 2 minutes. After adding 250  $\mu$ L of LB media, the cells were shaken at 37°C for 60 minutes at 225 rpm. The cells were poured onto the ampicillin containing LB agar plates and left overnight incubation.

For colony screening, 15 candidate colonies were picked up and screened against the proper insertion. For this, colonies were grown up into the 5 mL of LB media separately and then plasmid isolation was performed for each. Isolated plasmids were first checked out with PstI and HindIII double digestion and then verified by sequence analysis according to the conditions described in Table in 2.4 below. In this reaction commercial pQE2 sequencing primer (Qiagen, USA) was used and reaction was repeated at 35 cycles.

**Table 2.4 :** BigDye Terminator v3.1 cycle sequencing PCR (Roche, Switzerland).

Reagents	Volume ( $\mu$ L)	Reaction Conditions
BigDye Terminator v3.1	2	95°C 2 min
5x Sequencing Buffer	1	95°C 15 sec
Template	1	50°C 15 sec
Primer	1 (4pmol/ $\mu$ l)	60°C 4 min
H2O	5	4°C $\alpha$

The Sequencing PCR products purified by the following procedure. First, 50  $\mu$ L of EtOH in 95% concentration and 2  $\mu$ L Sodium Acetate were added onto 10  $\mu$ L of PCR product and incubated on ice for 15 minutes. Then, the mixture was centrifuged at



14000 rpm for 15 minutes and washed with 250  $\mu$ L of EtOH in 70% concentration. Then the mixture was centrifuge again at 14000 rpm for 15 minutes and let to dry at 95  $^{\circ}$ C. Finally, the sample was dissolved in 20  $\mu$ L HiDi-formamide and denatured at 95  $^{\circ}$ C for 5 minutes. After the final constructs obtained, PreScission Protease Cleavage (GE Healthcare, USA) site inserted between the histidine tag residue and AuBP2 via site-directed mutagenesis reaction by Invitrogen Site Directed Mutagenesis kit (Invitrogen) to remove histidine tag from either of the wild type and fusion protein. Primer sequences of site-directed mutagenesis reaction listed in Table 2.5 below.

**Table 2.5 :** Primer sequences of site-directed mutagenesis reaction.

	Primer Name	DNA Sequence
AuBP2-FDH	Forward Primer SDM_AuBP-FDH	5'CATGCGGGAGCTCAACTGGAAG TTCTGTTCCAGGGGCCCTGCGGCC CT T 3'
	Reverse Primer SDM_AuBP-FDH	5'TTGAGCTCCCGCATGCATATGG TGATG 3'
wt-FDH	Forward Primer SDM_wt-FDH	5'CATGCGGGAGCTCAACTGGAAG TTCTGTTCCAGGGGCCCATGAAG ATCGTTTTAG 3'
	Reverse Primer SDM_wt-FDH	5'TTGAGCTCCCGCATGCATATGG TGATG 3'

The PCR reaction was set up by mixing 5  $\mu$ L of 10X reaction buffer, 50 ng of dsDNA template, 125 ng of each forward and reverse primers and 1  $\mu$ L of dNTP mix. Then the ddH<sub>2</sub>O added onto reaction mixture to final volume of 50  $\mu$ L and started with 1  $\mu$ L of PfuTurbo DNA (Roche, Switzerland) polymerase addition. Reaction was start with initial denaturation step at 95 $^{\circ}$ C for 30 seconds and then amplification accomplished at 95 $^{\circ}$ C for 30 seconds, at 55 $^{\circ}$ C for 1 minute and at 68 $^{\circ}$ C for 5 minute respectively for 18 cycles.

### 2.2.3 Protein expression

Protein expression was performed in E.coli DH5 $\alpha$ -T1 cells (Invitrogen). Selected cell lines were grown in 100 mL LB including 100 mg/mL ampicillin overnight. After that culture was inoculated into 1000 mL LB including 100 mg/mL of ampicillin and

let them grow at 37°C, 200 rpm. When the culture optical density (OD) reaches to 0.5, protein expression was induced by IPTG to a final concentration of 0.5 mM. Induction was continued for 16°C for 16 hour to avoid possible inclusion body formation. After 16 hours of incubation cells are harvested by centrifugation at 5000 rpm for 10 minutes and pellet was stored at -20°C.

#### **2.2.4 Protein purification**

Protein purification performed according to QIAexpressionist (Qiagen, USA) protocol with slight modifications. In this protocol, firstly cell pellet was thawed on ice for 30 minutes and resuspended in lysis buffer at 2–5 mL per gram wet weight. Then 1 mg/mL of lysozyme added and incubated on ice for 45 minutes and finally sonicated. The obtained cell lysate was centrifuged at 10,000 x *g* for 30 minutes at 4°C to pellet the cellular debris. Then, the supernatant was transferred to a fresh tube and applied onto the Ni-NTA (Qiagen, USA) column which is previously equilibrated by Lysis Buffer and let it bind to the matrix for 5 minutes. The unspecific proteins removed by washing the coulumn first by Wash Buffer 1 and Wash Buffer 2 twice (ingredients are listed materials section, in appendix A). Finally, the protein of interest is eluted by 20 mL of Elution buffer.

Purified proteins were visualized by SDS-PAGE gel electrophoresis.

#### **2.2.5 Histidine tag removal**

Histidine residue before the AuBP2 sequence on purified protein was removed by using 10 µL of PreScission Protease for 1 mg of Histagged protein in 1X Cleavage buffer at 4°C for 30 minutes. Then, cleavage reaction was terminated by removing PreScission Protease from the reaction mixture via trapping by Glutathione Sepharose™ (GE Healthcare, USA) matrices and cleaved product was eluted by removing uncleaved histagged proteins via trapping by Ni-NTA matrices (Qiagen, USA).

Eluted non-histagged wtFDH and AuBP2-FDH were exchanged to 20mM Tris buffer (pH: 8.0) for further binding and kinetic activity measurement assays.

Protein concentration was calculated by Bradford Protein Assay in 595 nm, via Coomassie Brilliant Blue G-250 dye (Fermentas).

### **2.2.6 Kinetic activity assay**

Kinetic measurements were carried out with Biorad Benchmark Plus Microplate Reader at 25°C in a reaction mixture containing 20mM Tris Buffer at pH 8.0, 1mM NAD<sup>+</sup>, 0–40 mM formate and 0.4mM enzyme and analyzed based on Michealis-Menten equation by using GRAFIT Software.

### **2.2.7 Binding kinetics assay**

The binding kinetics of the AuBP2-FDH fusion proteins were examined by using Reichert SR7000 Single Channel SPR (Surface Plasmon Resonance). Freshly purified proteins were dissolved in 20 mM Tris buffer at pH 8.0 and immediately injected into a flow cell at a flow rate of 0.1 mL/min at 25°C for 10 minutes. Assuming Langmuir adsorption model, binding kinetics were estimated.



### 3. RESULTS AND DISCUSSION

#### 3.1 Gold Binding Peptide (AuBP) Selection and Characterization

Gold binding peptides were selected by our group previously in 2008. Different from the previously employed peptide selection processes, in Gold binding peptide selection FliTrx library (Invitrogen) was used in spite of M13 phage libraries (New England Biolabs) due to its several superiorities over M13 phage libraries like its shorter generation times and more simplified amplification/panning protocol.

During the selection process, there are 5 successful rounds of biopanning selection were employed and resulted 50 clones were further analyzed for binding affinities via fluorescence microscopy. Since the selected sequences did not converge toward a consensus sequence, the observed amino acid composition among strong, moderate, and weak binder groups of selected gold-binding sequences were compared with the native (unpanned) library to calculate the relative abundances of amino acids among them.

As a result, the two integral gold-binding peptide sequences (termed AuBP1 and AuBP2) were determined to use for further quantitative studies about their binding characteristics. Since the FliTrx-selected gold-binding sequences were originally displayed on bacterial cells as cyclic Cys-Cys disulfide loops, both cyclic and linear forms of AuBP1 and AuBP2 peptides were chosen to be characterized in order to be figure out the effect of cyclic conformation on binding affinity of peptides. The amino acid sequences, molecular weights (MW), isoelectronic focus points, and net charges of selected peptides are computed via ProtParam ([www.expasy.org](http://www.expasy.org)), shown in Figure 3.1 below.

**Table 3.1** : Amino acid sequences, MW, pI, and charges of selected peptides [73].

name	sequence	MW	pI	charge
l-AuBP1	WAGAKRLVLRRE	1454.7	11.7	+3

**Table 3.1 (continued) :** Amino acid sequences, MW, pI, and net charges of selected peptides [73].

name	sequence	MW	pI	charge
c-AuBP1	CGPWAGAKRLVLRREGPC	1967.3	9.7	+3
l-AuBP2	WALRRSIRRQSY	1591.8	12	+4
c-AuBP2	CGPWALRRSIRRQSYGPC	2106.4	10.7	+4

In order to assess binding properties of selected peptides SPR measurements were done. Data obtained from SPR experiments were fitted by least-squares regression to a 1:1 Langmuir adsorption model,

$$\theta(t-t_0) = \theta_{\infty}[1 - \exp(-k_{obs}(t-t_0))] \quad (3.1)$$

where  $\theta_{\infty}$  is the equilibrium surface coverage and  $k_{obs} = k_a C + k_d$ .

The adsorption rate ( $k_a$ ) and the desorption rate ( $k_d$ ) were calculated by determining  $k_{obs}$  at several concentrations. From these kinetic constants the equilibrium constant ( $K_{eq}$ ) and free energy change of adsorption ( $\Delta G$ ) were also calculated. The resulting kinetic constants ( $K_{eq}$ ,  $k_a$ ,  $k_d$ , and  $\Delta G$ ) are shown in Table 3.2.

**Table 3.2 :** The resulting kinetic constants of selected peptides [67, 73].

peptide	$K_{eq} \times 10^6 (M^{-1})$	$k_a \times 10^5 (M^{-1} s^{-1})$	$k_d \times 10^{-4} (s^{-1})$	$\Delta G_{ads} (kcal/mol)$
l-AuBP1	$3.24 \pm 1.31$	$1.32 \pm 0.21$	$41 \pm 8$	$-8.9 \pm 0.2$
c-AuBP1	$2.51 \pm 0.50$	$1.10 \pm 0.22$	$44 \pm 2$	$-8.7 \pm 0.1$
l-AuBP2	$2.34 \pm 0.34$	$1.00 \pm 0.03$	$43 \pm 5$	$-8.7 \pm 0.1$
c-AuBP2	$13.50 \pm 3.00$	$1.35 \pm 0.12$	$10 \pm 2$	$-9.7 \pm 0.2$

These results showed that all of l-AuBP1, c-AuBP1, and l-AuBP2 have almost the same binding properties. However, c-AuBP2 has an even significantly lower binding energy ( $-9.7 \pm 0.1$  kcal/mol) compared to others. This difference represents an order of magnitude higher equilibrium constant for c-AuBP2. The other fundamental difference in solid binding among these peptides is the desorption rate ( $k_d$ ), which is lower in c-AuBP2.

It is also very important that all of these SPR measurements done in bio-friendly, water-based solvents and thus it is quite clear that all of these four combinatorially selected AuBPs are a viable alternative to thiol-based systems that are employed in immobilization studies.

### 3.2 AuBP2-FDH Fusion Protein Construction

*cm*FDH and *c*-AuBP2 (**CGPWALRRSIRRQSYGPC**) sequences were used to construct AuBP2-FDH fusion protein.

Wild type FDH (wtFDH) sequence obtained into the pQE2 His-tag vector and AuBP2 sequence added onto the N-terminal of the wt-FDH. Since the AuBP2 sequence is too long to insert N-terminal of the FDH gene, we decided to perform two-step PCR by using four different forward and one reverse primer sequences as described in materials & methods sections. Map of constructed fusion protein and the molecular weights of constructed sequences are shown in Figure 3.1 and Table 3.3, respectively.

**Table 3.3 :** Fusion protein constructs and expected molecular weights.

Protein	Atomic mass unit (Dalton)
6xHis-pQE2-FDH	42027
6xHis-pQE2-AuBP2-FDH	44374
pQE2-FDH (cut)	40981
pQE2-AuBP2-FDH (cut)	43481

Finally, amplified PCR products visualized and verified by 1% agarose gel electrophoresis to check integrity and yield. Figure 3.2 below verifies the AuBP2-FDH amplification.

Since AuBP2-FDH fusion protein aimed to immobilize onto gold surface from AuBP2 region, we decided to insert a **GGGS** linker region between AuBP2 and wt-FDH sequences in order to provide flexibility to fusion protein. By first set of primer sequences, this flexible linker region was inserted.

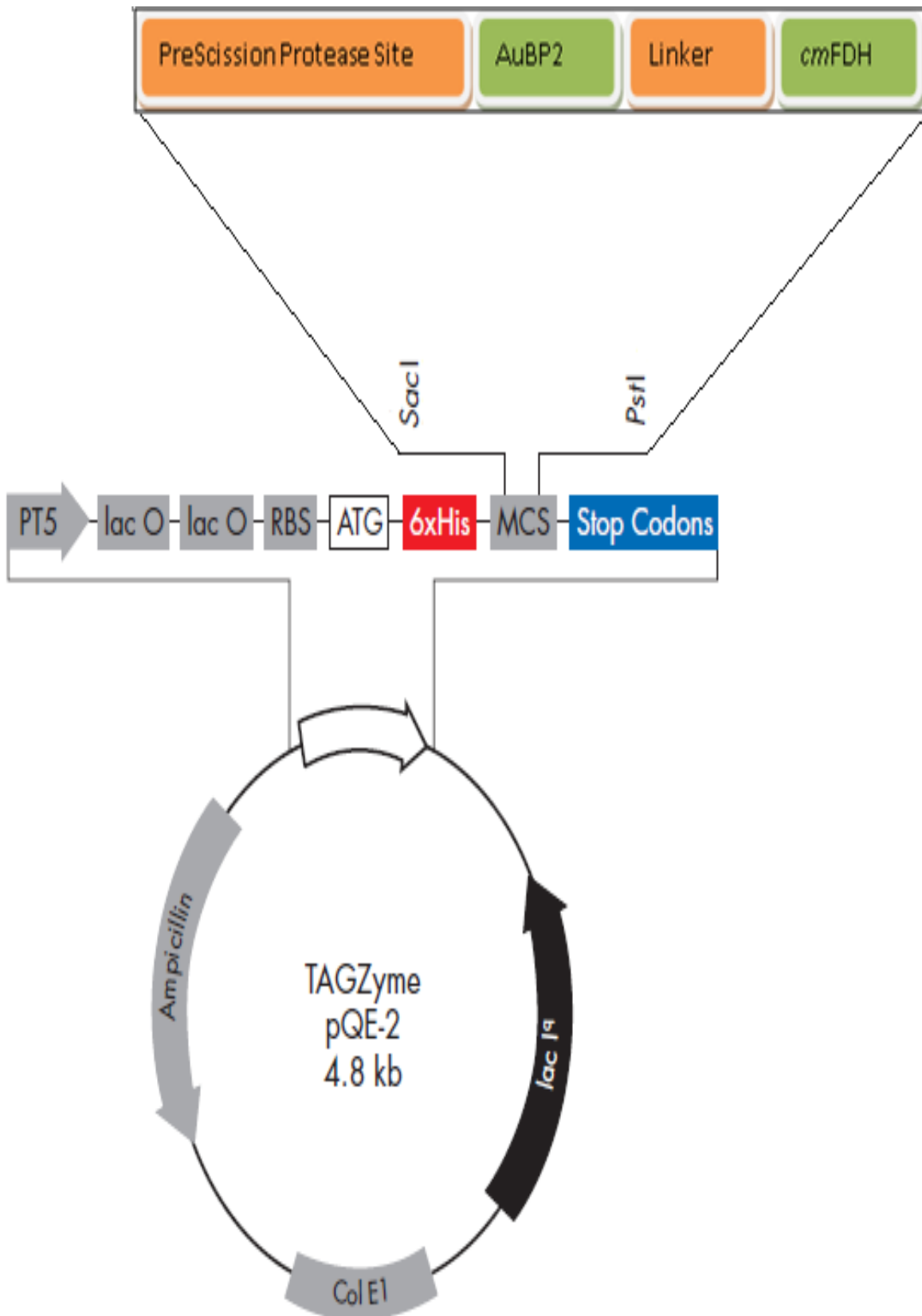


**Figure 3.1** : Schematic presentation of AuBP2-FDH fusion protein.



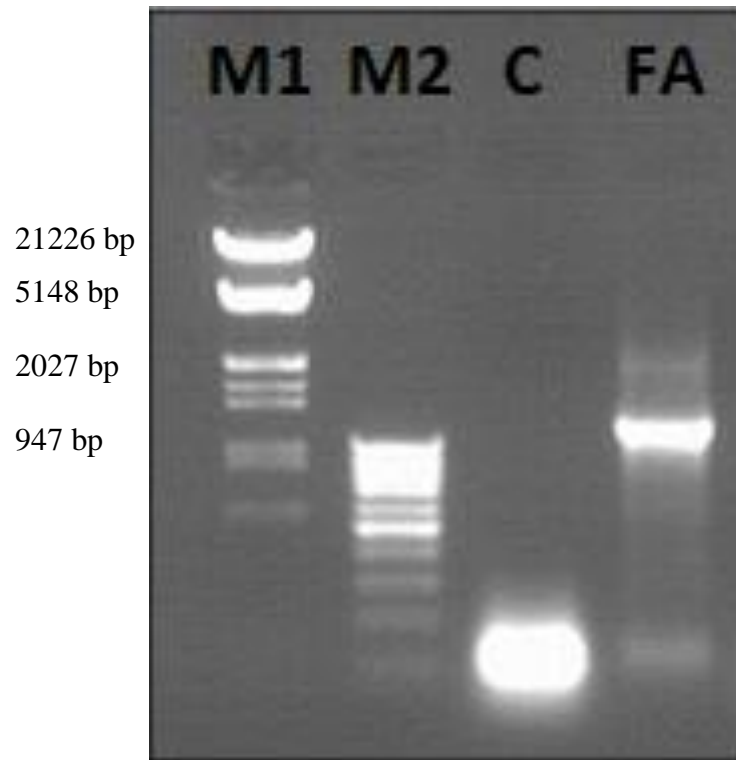


**Figure 3.2 :** Agarose gel (**M1, M2:** Marker, **C:**Control PCR **FA:** AuBP2-FDH). Amplified fragment was isolated from the gel and cloned into the pQE2 6xHis Expression vector. With this purpose, at first both constructed fragment and empty pQE2 plasmid vector was digested with PstI and SacI restriction enzymes. Figure 3.3 below verifies the true digestion.

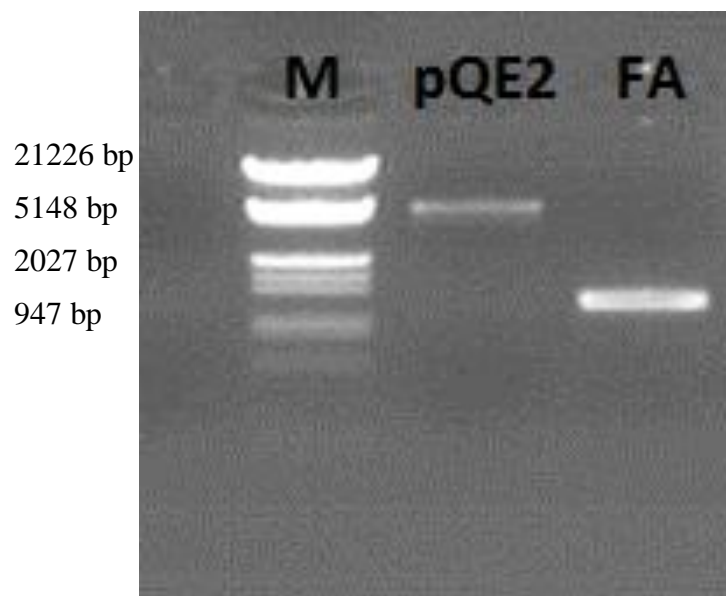


**Figure 3.3 :** Agarose gel (**M:** Marker 3, **pQE2:** digested pQE2, **FA:** amplified AuBP2-FDH).

Even though cloning efficiency is very low without sub-cloning the amplified fragment in TA cloning vector, we achieved to insert AuBP2-FDH sequence directly into the expression vector.

To avoid DNA loss, gel purification step skipped and reaction clean-up process performed to total digestion reaction by using Qiagen MinElute Reaction Cleanup kit (Qiagen, USA). Concentrations of the constructed fragment and empty pQE2 plasmid were determined by 1% agarose gel analysis again. Optimum plasmid template ratio was determined as 1.75 / 3.25 and ligation reaction was set up with Roche Rapid DNA Ligation kit (Roche, Switzerland).

### **3.3 Protein Expression**

Expression of both wtFDH and AuBP2-FDH performed in *E.coli* DH5 $\alpha$ -T1 cells according to the protocol described in methods section. Since expression of mutant forms of *cm*FDH when grew at 37°C causes to form inclusion bodies and lost half of their kinetic activities when grown at 30C, we choose to perform controlled and slow induction via 0.5 mM IPTG in final concentration at 16°C. Moreover, since expression rate of pQE2 promoter decreased dramatically at lower temperature, we continued induction process up to 16-18 hours to let cell produce enough AuBP2-FDH fusion protein.

### **3.4 Protein Purification**

Protein purification performed in NiNTA matrices (Qiagen, USA).

In order to avoid non-specific protein bindings caused by the ionic interactions between proteins and matrices, we made slight modifications on QIAexpressionist Ni-NTA purification protocol (Qiagen, USA). With this aim, we increase the imidazole concentration in lysis buffer 2-fold up to 20mM added and in wash buffer 2.5-fold up to 50mM to avoid non-specific bindings to NiNTA matrices. Moreover, we also added Triton X-100 ionic detergent into the wash buffer in order to get rid of contaminant proteins as a result of non-specific interactions between AuBP2-FDH fusion protein and foreign cellular proteins.

During the purification process flow through (FT), wash steps (W1, W2, W3) and elution (E1, E2, E3, E4) picked up as a separate fractions in order to obtain purist fraction. The visualization of these fractions can be seen in Figure 3.4 and Figure 3.5 for wtFDH and AuBP2-FDH, respectively. As it is seen in both Figure 3.4 and Figure 3.5 below, the obtained wtFDH and AuBP2-FDH enzymes are approximately 95% pure.

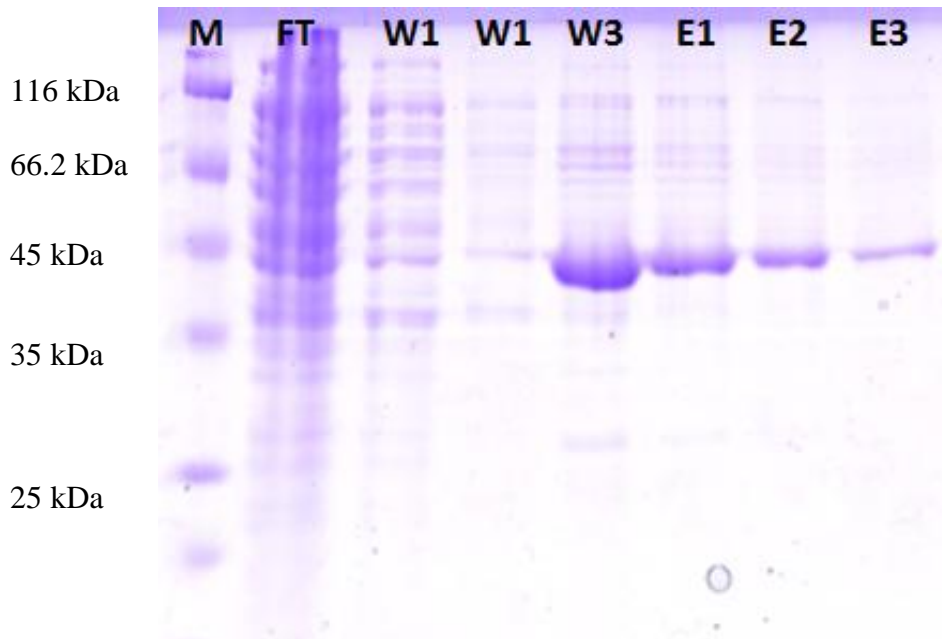


**Figure 3.4 :** SDS gel picture of wtFDH (M: Marker, FT: Flow through, W: Wash, E: Elute).

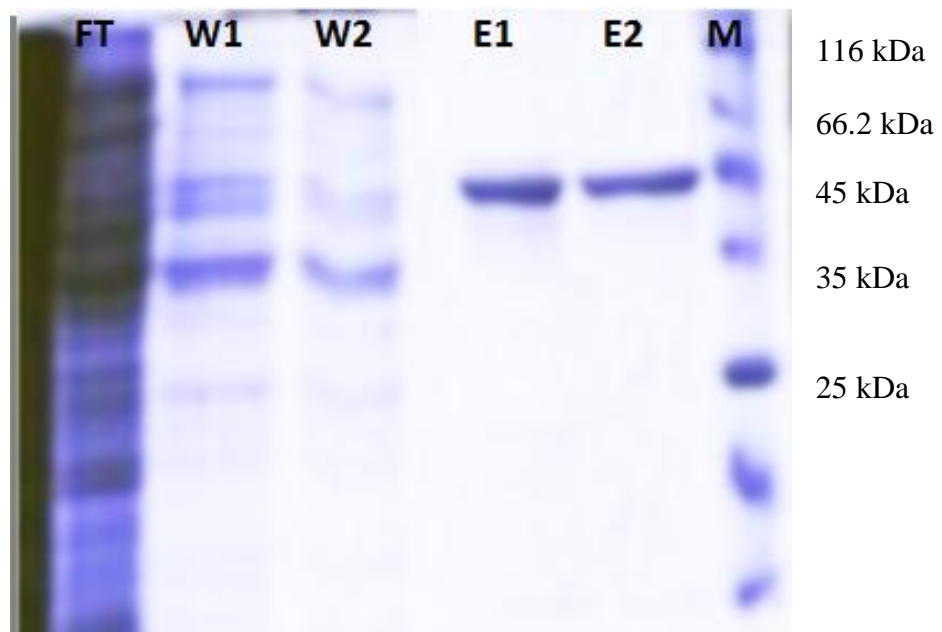


**Figure 3.5 :** SDS gel picture of AuBP2-FDH (FT: Flow through, W: Wash, E: Elute).

### 3.5 Histidine Tag Removal

The affinity of histidine residues inside the protein or in the N terminal histidine tag to gold surface has studied in detail in literature. For example, in the work of Belcher and co-workers, performed with the yeast surface display technique, 6xHistidine residue in both ends of the protein has shown distinct binding affinity toward a gold surface. In addition, the affinity of the imidazole ring in histidine amino acid for gold is further supported by the recent results that indicate that the adsorption of imidazole on gold nanoparticles results in self-assembled Au-imidazole complexes.

Parallel to these findings, we decided to remove histidine tail at the N-terminal of the both AuBP2-FDH and wt FDH by PreScission Protease Cleavage in order to prevent any interference of histidine tail to AuBP2 and possible false positive results in binding kinetics studies as a result of this interference.

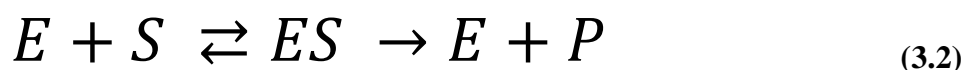
At this point it is very important to clarify that the choice of 6xHistag vector for the expression of both fusion and wild-type proteins is due the simplicity of the process. In the literature, there are several purification processes exists for formate dehydrogenase protein that are mainly based on column chromatograph. However, these chromatographic methods include at least 2 different step purification which mainly causes to a significant decrease in the yield of final product. By using 6xHistag expression vector systems, we could simply overcome this low yield problem and decrease the protein loss to a minimum level via purifying the enzyme by one-step process on NiNTA matrices. Moreover, it is also an important parameter for this decision that purity of final product is above 95 %.

The idea behind the use of PreScission Protease Cleavage rather than other commercial Histag removal systems is its simplicity. PreScission Protease Cleavage is a one step process which is carried out at 4°C and lasts only 30 minutes. With its unique simplicity and short reaction time, it is decided that PreScission Protease Cleavage is the best way for us to remove Histag from enzyme without any significant activity loss on enzyme. After the Histidine tag removal, wtFDH and AuBP2-FDH were exchanged to 20mM Tris buffer (pH: 8.0) immediately and protein concentration were calculated for further binding and kinetic activity measurement assays. Protein concentration calculated via Bradford Protein Assay in 595 nm, via Coomassie Brilliant Blue G-250 dye.

### 3.6 Kinetic Activity of AuBP2-FDH

There are several methods that have been proposed for enzyme activity measurement in literature. Among them, Michealis-Menten equation was chosen due to its simplicity and availability of examples where kinetic activity constants are determined via using this model.

In Michealis-Menten equation, a typical activity assay is carried out where the substrate concentration [S], is increased until the maximum velocity ( $V_{max}$ ) of the enzyme achieved which is called saturated state of enzyme. In this model, reaction rate is described as a number of reactions per second catalyzed per mole of the enzyme. The reaction rate increases with increasing substrate concentration [S], asymptotically approaching the maximum rate  $V_{max}$ . The Michaelis constant ( $k_m$ ) is the concentration of substrate in reaction solution, where the rate of the reaction is equal to the half of maximum velocity, called as substrate's affinity for the enzyme.  $K_m$  value is reversely proportional to substrate affinity so the higher  $K_m$  value gives lower affinity to substrate.  $k_{cat}/K_m$  values are used as a comparison data for efficiency of enzymes. The model of reaction used in Michealis-Menten equation is shown in equation below.



Assuming the enzyme concentration in reaction is much less than the substrate concentration, the general formula for Michealis-Menten is shown in equation below (3.3).

$$v = V_{max} \frac{[S]}{K_m + [S]} = k_{cat} [E_0] \frac{[S]}{K_m + [S]} \quad (3.3)$$

According to the model described above, the kinetic measurements were analyzed by using GRAFIT Software. First of all both mean velocity vs. substrate concentration and 1/mean velocity (1/V) vs. 1/substrate concentration (1/S) graphs were plotted for both wt-FDH and AuBP2FDH, seen in Figure 3.6, 3.7, 3.8, 3.9 below.

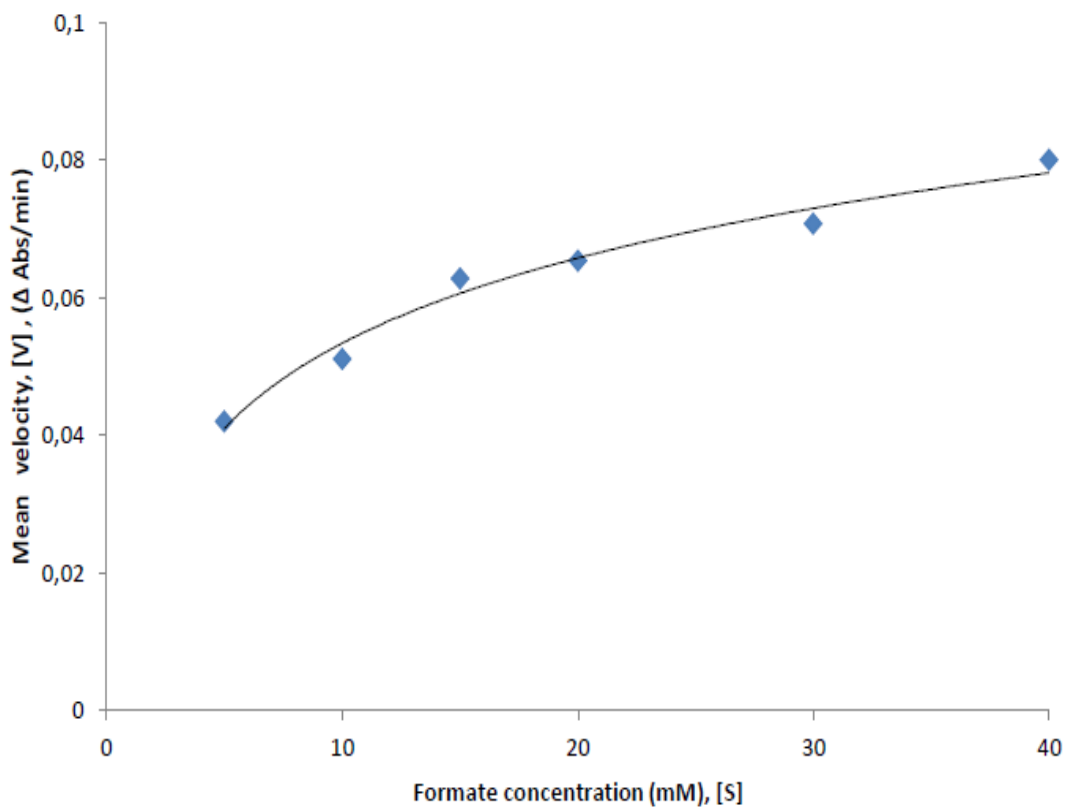


**Figure 3.6 :** Velocity vs substrate concentration graph of wt-FDH

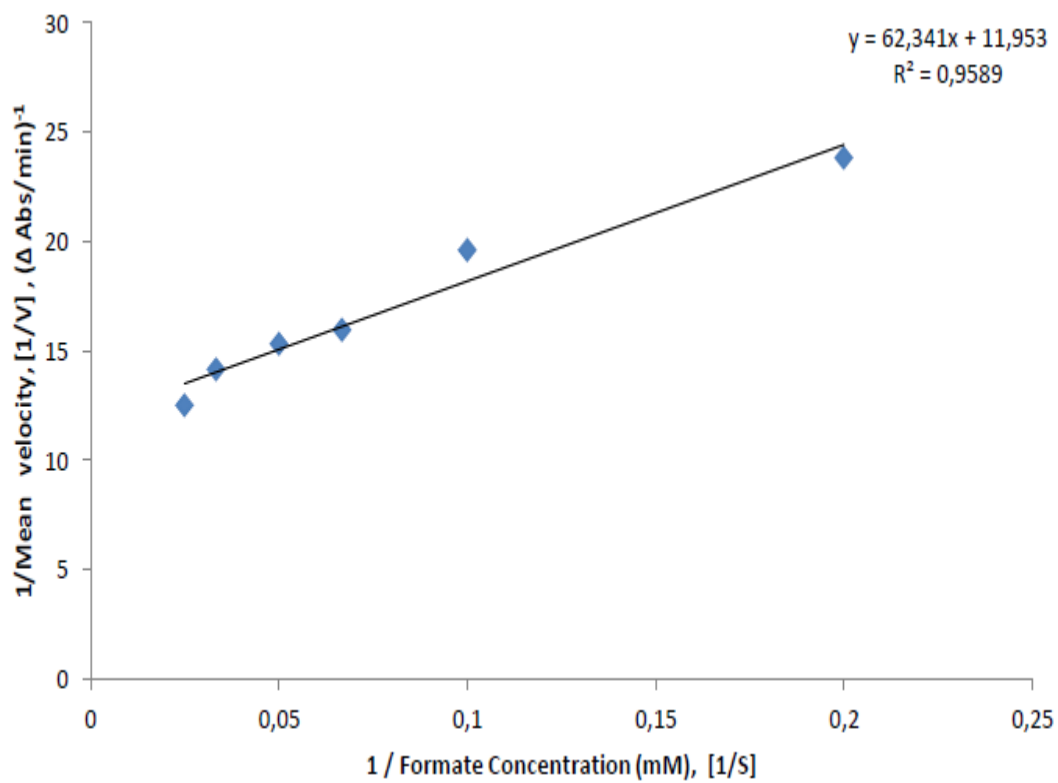


**Figure 3.7 :**  $(1/V)$  vs.  $(1/S)$  graph of wt-FDH

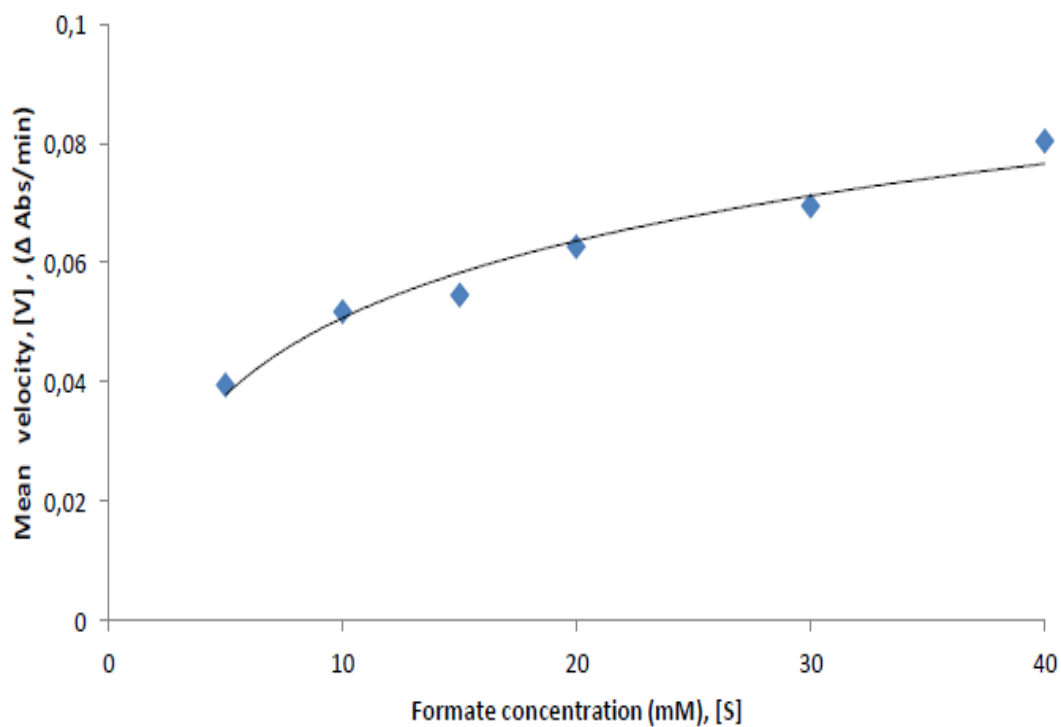


**Figure 3.8 :** Velocity vs substrate concentration graph of AuBP2-FDH

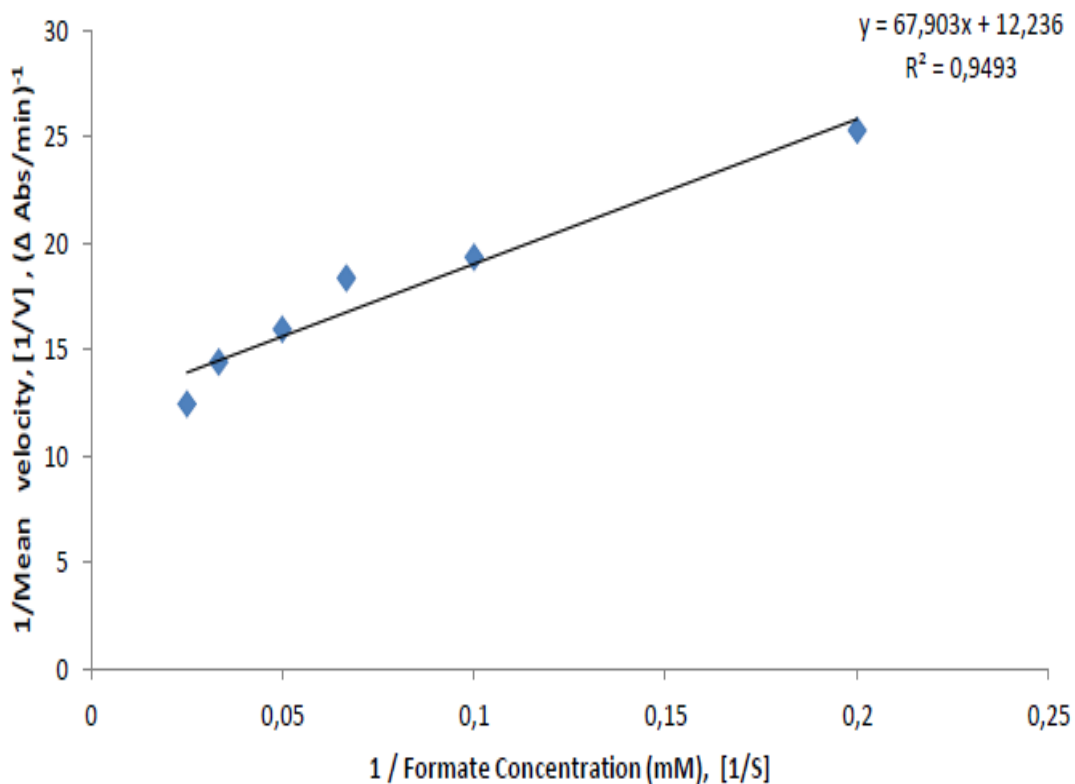


**Figure 3.9 :** (1/V) vs. (1/S) graph of AuBP2-FDH

After plotting the graphs for both wt-FDH and AuBP2-FDH kinetic parameters were calculated, Table 3.4. Calculated binding kinetics (Table 3.4) demonstrates that

addition of AuBP2 tag to the N-terminal of the FDH enzyme do not cause an activity loss in the enzyme. Difference between the catalytic activities of wtFDH and AuBP2 tagged FDH is negligible.

**Table 3.4 :** Activity constants of wt-FDH and AuBP2-FDH.

	Wt-FDH	AuBP2-FDH
$V_{\max}$ ( $\Delta$ Absorbance/minute)	$0,081 \pm 0,27$	$0,083 \pm 0,003$
$K_m$ (M)	5,54	5,21
$k_{\text{cat}}$ ( $s^{-1}$ )	0,547	0,56
$k_{\text{cat}}/K_m$ ( $s^{-1}M^{-1}$ )	0,098	0,107

This results show that AuBP2 is an ideal linker molecule in immobilization studies due to its inertness on enzyme activity in contrast to other linkers employed in conventional immobilization methods.

### 3.7 Binding Kinetics of wt-FDH and AuBP2-FDH

Here we used Surface Plasmon Resonance (SPR) spectroscopy to study the effect of engineered AuBP2 peptide attached to the N-terminal of the cmFDH protein. The apparent binding rates of AuBP2 were derived from non-linear curve fitting of the recorded SPR sensograms to the Langmuir binding isotherm as described earlier with a model, equation (3.1). The fits and resulting kinetic constants ( $k_a$ ,  $k_d$ ,  $k_a/k_d$ ) are shown in Figure 2 and Table 2, respectively.

**Table 3.5 :** Binding Constants of wt-FDH and AuBP2-FDH

	wt-FDH	AuBP2-FDH
$k_a$ ( $M^{-1}s^{-1}$ )	$2,38 \cdot 10^{-3}$	$10,35 \cdot 10^{-3}$
$k_d$ ( $s^{-1}$ )	$1,96 \cdot 10^{-3}$	$0,665 \cdot 10^{-3}$
$k_a/k_d$ ( $M^{-1}$ )	1,214	15,564



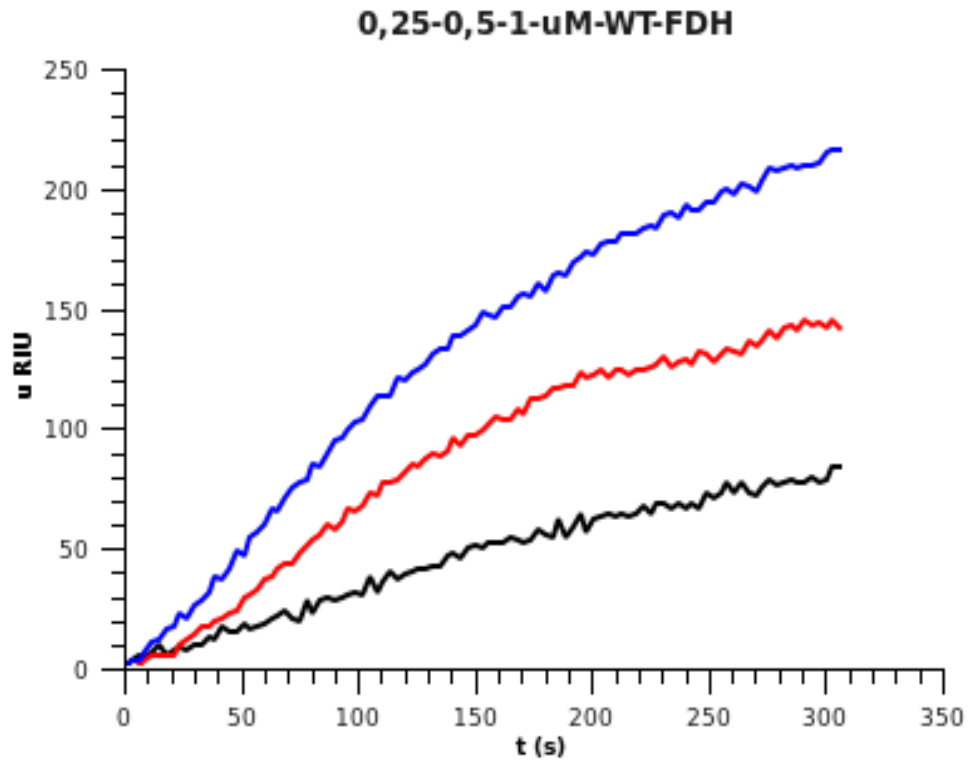


**Figure 3.10** : SPR sensogram of wt-FDH.

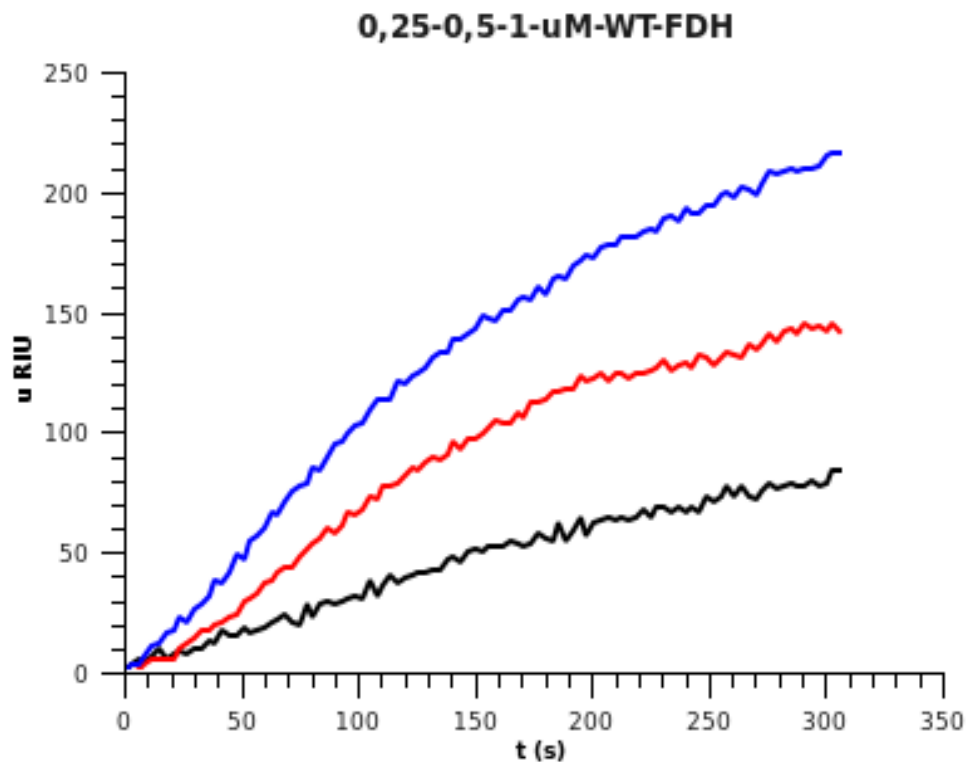


**Figure 3.11** : SPR sensogram of AuBP2-FDH.

As expected, both of the wild type FDH and AuBP-FDH fusion protein bind to the gold surface but with quite different the binding characteristics. The binding affinity of wild type FDH to gold surface, albeit it is quite lower than fusion protein, can

explained by histidine and cysteine residues exist on the surface of the protein, shown in Figure 3.12.

The affinity of histidine and cysteine residues to gold surface via their functional imidazole and -SH groups respectively results with an adsorption of wild type protein on gold surface to a certain level. Moreover, it is also possible that the -NH<sub>2</sub> groups flipped from the enzyme toward gold surface are contribute this interaction with some degree.

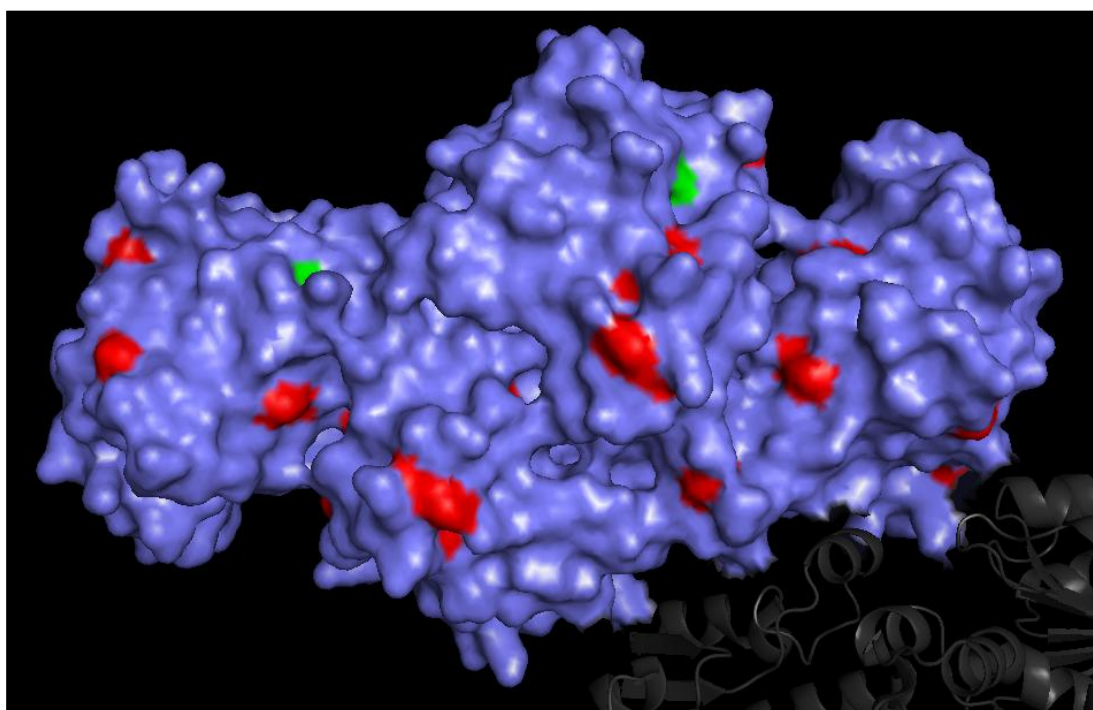


**Figure 3.12 :** Surface display of *cbFDH* (Histidine and Cysteine residues are shown in red and green color, respectively).

However, as it can be seen from the Table 3.5 above, there is a significant amount of difference between both the adsorption and desorption rates of wild type FDH and AuBP-FDH, both of which leads to higher  $k_a/k_d$  values for AuBP2-FDH than AuBPs. It can be simply proposed that the effect of AuBP2, as an efficient surface linker for FDH, resulted in 12-fold increase in the adsorption behavior of FDH on gold surface with high surface coverage.

#### **4. CONCLUSIONS AND FUTURE PERSPECTIVES**

Controlling the orientation of enzyme on the support surface has always been a big challenge in enzyme immobilization studies. In this study, we mainly aimed to develop a multifunctional enzyme, which can immobilize or self-assemble on the inorganic material surface with great of material specificity and at a very close proximity. However, conventional immobilization technologies are far from meeting these needs and expectations due to their significant drawbacks, which are discussed in introduction section.

At this point, we thought an alternative strategy needed and GEPI-mediated immobilisation opened us a novel route by its great potential to overcome all these aforementioned drawbacks and to meet our needs in enzyme immobilization technology.

In this study, we chose NAD<sup>+</sup>-dependent formate dehydrogenase as a model enzyme due to its industrial importance and we chose gold surface due to its wide range of application areas. From more specific point of view, the purpose of this study is to construct AuBP2-FDH fusion enzyme and characterize the multifunctional properties, and finally demonstrate the effects of AuBP2 conjugation on binding and kinetic properties of FDH enzyme on both soluble and immobilized forms on the gold surface.

With this aim, previously selected cyclic-AuBP2 gold binding peptide is chose among other gold binding peptides and decided to employ due to its superior binding properties on gold surface. Moreover, we chose *Candida methylica* NAD<sup>+</sup>-dependent formate dehydrogenase enzyme as a model among the other homologs of the NAD<sup>+</sup>-dependent formate dehydrogenase isolated from various species due to the availability of information about the purification, kinetic activity and stability of enzyme.

Moreover, histidine tag derived single step purification process for *Candida methylica* NAD<sup>+</sup>-dependent formate dehydrogenase is previously achieved by

colloquies and this serves us an important advantage to overcome laborious and low yield purification processes.

To assess our GEPI-based immobilization approach or in other words to bring in a strong and very specific surface affinity to *Candida methylica* NAD<sup>+</sup>-dependent formate dehydrogenase, we constructed a bi-functional enzyme by adding AuBP2 peptide sequence onto the N-terminal of the *Candida methylica* NAD<sup>+</sup>-dependent formate enzyme. We also separated these peptide and enzyme with a GGGS linker region to give flexibility to novel bi-functional enzyme. Then, we successfully achieved to overexpress the enzyme in by using *E.coli* expression system and purified on Ni-NTA matrices. Next, we characterized its kinetic and binding properties by kinetic activity assay and SPR spectroscopy, respectively.

Albeit we tried to overcome the formation of inclusion bodies during the expression process, the use of bacterial expression system to produce the cmFDH enzyme served us several benefits such as, low production costs, simple and time efficient expression. We prevent the formation of inclusion bodies by decreasing the induction temperature from 37<sup>0</sup>C to 16<sup>0</sup>C and inducer concentration from 1mM to 0.5 mM. Low temperature and inducer concentration enables to slow down the expression and give time to newly expressed proteins to fold in correctly and thus, prevent inclusion body formation. In order to compensate the decrease in the level of expression and to obtain high yield, we increased the induction time from 4 hours up to 16-18 hours.

In the purification process, we slightly modified the suggested protocol in the QIAexpressionist (Qiagen, USA) manual in order to increase the purity of the enzyme. There are two main limitations of the QIAexpressionist His-tag purification protocol which are unspecific protein binding to the NiNTA matrix due the presence of high histidine containing proteins and unspecific protein-protein binding which is usually caused by intermolecular interactions between proteins. These two limitations are caused by the decrease in the efficiency of the purification process. To overcome unspecific protein binding to the NiNTA matrices we increased the amount of the concentration of imidazole in both lysis and wash buffers. Additionally, we also added Triton X-100 non-ionic detergent into the wash buffers to prevent unspecific protein-protein interactions. For the next step of the purification, we cut out his-tag residue of the proteins locating in N-terminal end. Since the histidine is an imidazole containing amino acid which has the ability to

interact with gold surface we thought that this interaction might contribute to the binding affinity of the protein or cause to interact with gold surface in an unspecific manner and thus, lead to false positive results. Moreover, the location of his-tag residue was a potential problem for this study. Since it was located in front of the AuBP2 region, it may hinder the effect of AuBP2 on protein binding and might lead to true negative results too.

Kinetic properties of both wt-FDH and AuBP2-FDH were analyzed by kinetic activity assays and obtained results were amazing. As a negative control, we calculated the kinetic activity parameters of wt-FDH and compare them with kinetic activity parameters of AuBP2-FDH to see the effect of AuBP2 conjugation over enzyme activity. AuBP2 addition results with a negligible amount of increase in  $k_m$  and decrease in  $k_{cat}$  values. The calculated catalytic efficiencies ( $k_{cat}/k_m$ ) of wt-FDH and AuBP2-FDH are 0,107 and 0,098, respectively. Based on these kinetic activity measurements, it demonstrated that FDH enzyme when it is conjugated to AuBP2 preserved its catalytic activity, over 90% without any significant loss.

To assess the binding characteristics of the wt-FDH and AuBP2-FDH we performed SPR experiments and calculated the binding constants. AuBP2 conjugated FDH enzyme has an order of magnitude with a  $k_a/k_d$  value equal to 15,564 M<sup>-1</sup> whereas the wt-FDH with 1,214 M<sup>-1</sup>. These results demonstrate that AuBP2 conjugation of FDH enzyme lead to 12-fold increase in the affinity of enzyme to gold surface.

From the both binding affinity and catalytic activity sides our results show that AuBP2 peptide conjugation brought in very specific gold binding affinity to FDH enzyme up to 12 fold without any significant effect on its catalytic activity. More importantly, all of these experiments are performed under physiological conditions, which show us AuBP2 is an ideal, bio-friendly linker molecule for enzyme studies.

The design of bio-friendly systems is at the core of nanotechnology and science. This study will open a new route for enzyme immobilization studies under biological conditions. Moreover, in terms of wide range of application areas of enzymes, which are mostly used in immobilized form, it is very clear that this study will make a big impact on different fields from sensing technologies to energy technologies.



## REFERENCES

- [1] **Tishkov, V.I., and Popov, V.O.** (2006). Protein engineering of formate dehydrogenase, *Biomolecular Engineering*, **23(2-3)**, 89-110.
- [2] **Allen, S.J., and Holbrook, J.J.** (1995). Isolation, sequence and overexpression of the gene encoding NAD-dependent formate dehydrogenase from the methylotrophic yeast *Candida methylica*, *Gene*, **162(1)**, 99-104.
- [3] **Kula, M.R., and Wandrey, C.** (1987). Continuous enzymatic transformation in an enzyme-membrane reactor with simultaneous NADH regeneration, *Methods in Enzymology*, (**17**), 9-21.
- [4] **Wichmann, R.** (1981). Continuous enzymatic transformation in an enzyme membrane reactor with simultaneous NAD(H) regeneration, *Biotechnology and Bioengineering*, **23(12)**, 2789-2802.
- [5] **Baba, T.** (2002). Genome and virulence determinants of high virulence community-acquired MRSA, *The Lancet*, **359(9320)**, 1819-1827.
- [6] **Li, L.L.** (2005). The complete genome sequence of Mycobacterium avium subspecies paratuberculosis, *Proceedings of the National Academy of Sciences of the United States of America*, **102(35)**, 12344-12349.
- [7] **Parkhill, J.** (2003). Comparative analysis of the genome sequences of Bordetella pertussis, Bordetella parapertussis and Bordetella bronchiseptica, *Nature Genetics* **35(1)**, 32-40.
- [8] **Cazalet, C., et al.** (2004). Evidence in the Legionella pneumophila genome for exploitation of host cell functions and high genome plasticity, *Nature Genetics*, **36(11)**, 1165-1173.
- [9] **Chien, M.C.** (2004). The genomic sequence of the accidental pathogen Legionella pneumophila, *Science*, **305(5692)**, 1966-1968.
- [10] **Hwang, L.** (2003). Identifying phase-specific genes in the fungal pathogen Histoplasma capsulatum using a genomic shotgun microarray, *Molecular Biology of the Cell*, **14(6)**, 2314-2326.
- [11] **Loftus, B.J.** (2005). The genome of the basidiomycetous yeast and human pathogen Cryptococcus neoformans, *Science*, **307(5713)**, 1321-1324.
- [12] **Tishkov, V.I.** (1993). Catalytic Properties and Stability of a Pseudomonas sp.101 Formate Dehydrogenase Mutants Containing Cys-255-Ser and Cys-255-Met Replacements, *Biochemical and Biophysical Research Communications*, **192(2)**, 976-981.
- [13] **Lamzin, V.S.** (1994). High Resolution Structures of Holo and Apo Formate Dehydrogenase, *Journal of Molecular Biology*, **236(3)**, 759-785

- [14] **Weerasinghe, P.A., Weerasekera, M., and Van Holm, L.H.J.** (1999). Use of isoenzymes to differentiate growth categories of *Pericopsis mooniana* trees, *Biologia Plantarum*, **42(40)**, 541-547.
- [15] **Resch, A.** (2005). Differential gene expression profiling of *Staphylococcus aureus* cultivated under biofilm and planktonic conditions, *Applied and Environmental Microbiology*, **71(5)** 2663-2676.
- [16] **Hummel, W., and Kula, M.R.** (1989). Dehydrogenases for the synthesis of chiral compounds, *European Journal of Biochemistry*, **184(1)**, 1-13.
- [17] **Liese, A.** (1999). Production of fine chemicals using biocatalysis, *Current Opinion in Biotechnology*, **10(6)**, 595-603.
- [18] **Bommarius, A.S.** (1995). Synthesis and use of enantiomerically pure tert-leucine, *Tetrahedron: Asymmetry*, **6(12)**, 2851-2888.
- [19] **Debnam, P.M.** (1997). Colorimetric assay for substrates of NADP(+)-dependent dehydrogenases based on reduction of a tetrazolium dye to its soluble formazan, *Analytical Biochemistry*, **250(2)**, 253-255.
- [20] **Andreadeli, A.** (2008). Structure-guided alteration of coenzyme specificity of formate dehydrogenase by saturation mutagenesis to enable efficient utilization of NADP(+), *Febs Journal*, **275(15)**, 3859-3869.
- [21] **Chen, R.D.** (1996). Redesigning secondary structure to invert coenzyme specificity in isopropylmalate dehydrogenase, *Proceedings of the National Academy of Sciences of the United States of America*, **93(22)**, 12171-12176.
- [22] **Lamzin, V.S.** (1992). Crystal-structure of NAD-dependent formate dehydrogenase, *European Journal of Biochemistry*, **206(2)**, 441-452.
- [23] **Chen, R.D.** (1999). A general strategy for enzyme engineering, *Trends in Biotechnology*, **17(9)**, 344-345.
- [24] **Chen, R.D.** (2001). Enzyme engineering: rational redesign versus directed evolution, *Trends in Biotechnology*, **19(1)**, 13-14.
- [25] **Dalby, P.A.** (2011). Strategy and success for the directed evolution of enzymes, *Current Opinion in Structural Biology*, **21(4)**, 473-480.
- [26] **Rusmini, F., Zhong, Z., and Feijen, J.** (2007). Protein immobilization strategies for protein biochips, *Biomacromolecules*, **8(6)**, 1775-1789.
- [27] **Fuentes, M.** (2004). Reversible and strong immobilization of proteins by ionic exchange on supports coated with sulfate-dextran, *Biotechnol Prog*, **20(4)**, 1134-1139.
- [28] **Piletsky, S.** (2003). Surface functionalization of porous polypropylene membranes with polyaniline for protein immobilization, *Biotechnol Bioeng*, **82(1)**, 86-92.
- [29] **Yam, C.M.** (2006). Preparation, characterization, resistance to protein adsorption, and specific avidin-biotin binding of poly (amidoamine) dendrimers functionalized with oligo(ethylene glycol) on gold, *J Colloid Interface Sci*, **296(1)**, 118-130.



- [30] **Jiang, K.Y.** (2004). Protein immobilization on carbon nanotubes via a two-step process of diimide-activated amidation, *Journal of Materials Chemistry*, **14(1)**, 37-39.
- [31] **Linqiu, C.** (2005). Immobilised enzymes: science or art, *Current Opinion in Chemical Biology*, **(9)**, 217–226
- [32] **Tischer, W.** (1999). Immobilized enzymes: Methods and applications, *Biocatalysis*, **200**, 95-126.
- [33] **Patel, N.** (1997). Immobilization of protein molecules onto homogeneous and mixed carboxylate-terminated self-assembled monolayers, *Langmuir*, **13(24)**, 6485-6490.
- [34] **Yan, M.D.** (1993). Photochemical functionalization of polymer surfaces and the production of biomolecule-carrying micrometer-scale structures by deep-uv lithography using 4-substituted perfluorophenyl azides, *J Am Chem Soc*, **115(2)**, 814-816.
- [35] **Betancor, L.** (2006). Different mechanisms of protein immobilization on glutaraldehyde activated supports: Effect of support activation and immobilization conditions, *Enzyme Microb Technol*, **39(4)**, 877-882.
- [36] **Choi, H.J.** (2005). Micropatterning of biomolecules on glass surfaces modified with various functional groups using photoactivatable biotin, *Anal Biochem*, **347(1)**, 60-66.
- [37] **D'Souza, S.F., and Godbole, S.S.** (2002). Immobilization of invertase on rice husk using polyethylenimine, *J Biochem Biophys Methods*, **52(1)**, 59-62.
- [38] **MacBeath, G., and Schreiber, S.L.** (2000). Printing proteins as microarrays for high-throughput function determination, *Science*, **289(5485)**, 1760-1763.
- [39] **Jongsma, M.A., and Litjens, R.** (2006). Self-assembling protein arrays on DNA chips by auto-labeling fusion proteins with a single DNA address, *Proteomics*, **6(9)**, 2650-2655.
- [40] **Gauvreau, V.** (2004). Engineering surfaces for bioconjugation: Developing strategies and quantifying the extent of the reactions, *Bioconjug Chem*, **15(5)**, 1146-1156.
- [41] **Viitala, T., Vikholm, I., and Peltonen, J.** (2000). Protein immobilization to a partially cross-linked organic monolayer, *Langmuir*, **16(11)**, 4953-4961.
- [42] **Masri, M.S., and Friedman, M.** (1988). Protein reactions with methyl and ethyl vinyl sulfones, *J Protein Chem*, **7(1)**, 49-54.
- [43] **Lutolf, M.P., and Hubbell, J.A.** (2003). Synthesis and physicochemical characterization of end-linked poly(ethylene glycol)-co-peptide hydrogels formed by Michael-type addition, *Biomacromolecules*, **4(3)**, 713-722. 57
- [44] **Fernandezlafuente, R.** (1993). Preparation of activated supports containing low pk amino-groups - a new tool for protein immobilization via the carboxyl coupling method, *Enzyme Microb Technol*, **15(7)**, 546-550.

- [45] **Collioud, A.** Oriented and covalent immobilization of target molecules to solid supports - synthesis and application of a light-activatable and thiol-reactive cross-linking reagent, *Bioconjug Chem*, **4(6)**, 528-536.
- [46] **Blawas, A.S. and W.M. Reichert**, Protein patterning. *Biomaterials*, 1998. 19(7-9): p. 595-609.
- [47] **Sigrist, H.** (1995). Surface immobilization of biomolecules by light, *Optical Engineering*, **34(8)**, 2339-2348.
- [48] **Lesaicherre, M.L.** (2002). Developing site-specific immobilization strategies of peptides in a microarray, *Bioorganic & Medicinal Chemistry Letters*, **12(16)**, 2079-2083.
- [49] **Tam, J.P., Xu, J.X., and Eom, K.D.** (2001). Methods and strategies of peptide ligation, *Biopolymers*, **60(3)**, 194-205.
- [50] **Zhen, G.L.** (2006). Nitrilotriacetic acid functionalized graft copolymers: A polymeric interface for selective and reversible binding of histidine-tagged proteins, *Advanced Functional Materials*, **16(2)**, 243-251.
- [51] **Lata, S.** (2005). High-affinity adaptors for switchable recognition of histidine-tagged proteins, *J Am Chem Soc*, **127(29)**, 10205-10215.
- [52] **Wegner, G.J.** (2003). Fabrication of histidine-tagged fusion protein arrays for surface plasmon resonance imaging studies of protein-protein and protein-DNA interactions, *Anal Chem*, **75(18)**, 4740-4746.
- [53] **Schmid, E.L.** (1997). Reversible oriented surface immobilization of functional proteins on oxide surfaces. *Anal Chem*, 1997. 69(11): p. 1979-1985.
- [54] **Gershon, P.D., and Khilko, S.** (2000). Stable chelating linkage for reversible immobilization of oligohistidine tagged proteins in the biacore surface-plasmon resonance detector, *Journal of Immunological Methods*, **183(1)**, 65-76.
- [55] **Wang, Z.H., and Jin, G.** (2003). Feasibility of protein A for the oriented immobilization of immunoglobulin on silicon surface for a biosensor with imaging ellipsometry, *J Biochem Biophys Methods*, **57(3)**, 203-211.
- [56] **Lu, B., Smyth, M.R., and Okennedy, R.** (1996). Oriented immobilization of antibodies and its applications in immunoassays and immunosensors, *Analyst*, **121(3)**, R29-R32.
- [57] **Lee, S.Y.,** (2011). Inorganic nanomaterial-based biocatalysts, *Bmb Reports*, **44(2)**, 77-86.
- [58] **Wu, C.** (2008). An enzymatic kinetics investigation into the significantly enhanced activity of functionalized gold nanoparticles, *Chem Commun (Camb)*, **2008(42)**, 5327-5329.
- [59] **Villalonga, R., Cao, R., and Fragoso, A.** (2007). Supramolecular chemistry of cyclodextrins in enzyme technology, *Chemical Reviews*, **107(7)**, 3088-3116.
- [60] **Mazur, M.** (2007). Immobilization of laccase on gold, silver and indium tin oxide by zirconium-phosphonate-carboxylate (ZPC) coordination chemistry, *Bioelectrochemistry*, **71(1)**, 15-22.

- [61] Laszlo, J.A., and Evans, K.O. (2007). Influence of self-assembled monolayer surface chemistry on *Candida antarctica* lipase B adsorption and specific activity, *Journal of Molecular Catalysis B-Enzymatic*, **48(3-4)**, 84-89.
- [62] Jia, H.F., Zhu, G.Y., and Wang, P. (2003). Catalytic behaviors of enzymes attached to nanoparticles: The effect of particle mobility, *Biotechnol Bioeng*, **84(4)**, 406-414.
- [63] Kresge, C.T. (1992). Ordered mesoporous molecular-sieves synthesized by a liquid-crystal template mechanism, *Nature*, **359(6397)**, 710-712.
- [64] Tamerler, C. (2010). Molecular Biomimetics: GEPI-Based Biological Routes to Technology, *Biopolymers*, **94(1)**, 78-94.
- [65] Tamerler, C., and Sarikaya, M. (2009). Molecular biomimetics: nanotechnology and bionanotechnology using genetically engineered peptides, *Philosophical Transactions of the Royal Society* **367(1894)**, 1705-1726.
- [66] Tamerler, C., and Sarikaya, M. (2008). Genetically Designed Peptide-Based Molecular Materials, *ACS Nano*, **3(7)**, 1606-1615.
- [67] Hnilova, M. (2009). Effect of Molecular Conformations on the Adsorption Behavior of Gold-Binding Peptides, *Langmuir*, **24(21)**, 12440-12445.
- [68] Tamerler, C. and Sarikaya, M., (2007). Molecular biomimetics: Utilizing nature's molecular ways in practical engineering, *Acta Biomater*, **3(3)**, 289-299.
- [69] Tamerler, C. (2007). Genetically engineered polypeptides for inorganics: A utility in biological materials science and engineering, *Materials Science and Engineering: C*, **27(3)**, 558-564.
- [70] Tamerler, C. (2003). Biomimetic multifunctional molecular coatings using engineered proteins, *Progress in Organic Coatings*, **47(3-4)**, 267-274.
- [71] Brown, S., Sarikaya, M., and Johnson, E. (2000). A genetic analysis of crystal growth, *J Mol Biol*, **299(3)**, 725-735.
- [72] Sarikaya, M. (2003). Molecular biomimetics: nanotechnology through biology, *Nat Mater*, **2(9)**, 577-585.
- [73] Hnilova, M. (2012). Single-step fabrication of patterned gold film array by an engineered multi-functional peptide, *J Colloid Interface Sci*, **365(1)**, 97-102.
- [74] Tang, Y., Zeng, X., and Liang, J. (2010). Surface Plasmon Resonance: An Introduction to a Surface Spectroscopy Technique, *Journal of Chemical Education*, **87(7)**, 742-746.
- [75] Willets, K.A., and Van Duyne, R.P. (2007). Localized surface plasmon resonance spectroscopy and sensing, *Annual Review of Physical Chemistry*, **(7)**, 267-297.
- [76] Karpovich, D.S., and Blanchard, G.J. (1994). Direct measurement of the adsorption-kinetics of alkanethiolate self-assembled monolayers on a microcrystalline gold surface, *Langmuir*, **10(9)**, 3315-3322.

- [77] **Kacar, T.** (2009). Directed Self-Immobilization of Alkaline Phosphatase on Micro-Patterned Substrates Via Genetically Fused Metal-Binding Peptide, *Biotechnol Bioeng*, **103(4)**, 696-705.
- [78] **Love, J.C.** (2005). Self-assembled monolayers of thiolates on metals as a form of nanotechnology, *Chemical Reviews*, **105(4)**, 1103-1169.

## **APPENDICES**

**APPENDIX A:** Materials

**APPENDIX B:** Laboratory equipments

## **APPENDIX A : Materials**

### **Luria Bertani (LB) Medium**

10 g tryptone (Acumedia), 5 g yeast extract (Acumedia), 5 g NaCl (Riedel-de-Haen) were dissolved in distilled water and completed up to 1 L. The pH was adjusted to 7.0-7.5 with 5 M NaOH and sterilized for 15 minutes under 1.5 atm at 121 °C. The medium was stored at room temperature.

### **LB Agar Medium**

10 g tryptone (Acumedia), 5 g yeast extract (Acumedia), 5 g NaCl (Riedel-de-Haen) and 15 g bactoagar (Merck) were dissolved in distilled water up to 1 L and the pH is adjusted to 7.0 with 5 M NaOH. Media is sterilized by autoclaving for 15 min at 121 °C. The medium was poured to the plates.

### **SOC Medium**

20 g tryptone, 5 g yeast extract and 0.5 g NaCl were dissolved in distilled water. 10 mL of 250 mM KCl was added to the solution and the pH was adjusted to 7.0 with 5 M NaOH. Volume was adjusted to 1 L with distilled water and the solution was autoclaved. 10 mM MgCl<sub>2</sub> and 20 mM glucose were added just before the usage of media.

### **Ampicilline Stock Solution**

100 mg Ampicillin (Sigma) was dissolved in 1 mL deionized water, sterilized by filtration using 0.22 µm filter. This stock solution was used in LB medium with 1:1000 dilution rate.

### **Lysis Buffer**

6.90 g NaH<sub>2</sub>PO<sub>4</sub>•H<sub>2</sub>O , 17.54 g NaCl, and 1.36 g imidazole were dissolved in distilled water up to 1 L with a final concentrations of 50 mM, 300 mM, and 20 mM, respectively. The pH is adjusted to 8.0 with 5 M NaOH and sterilized by autoclaving for 15 min at 121 °C.

### **X-gal Stock Solution**

80 mL glycerol (Riedel-de-Haen) and 20 mL distilled water were mixed to give 80 % (v/v) solution and sterilized for 15 min at 121 °C.

### Wash 1 Buffer

6.90 g  $\text{NaH}_2\text{PO}_4 \cdot \text{H}_2\text{O}$  , 17.54 g NaCl, and 1.36 g imidazole were dissolved in distilled water up to 1 L with a final concentrations of 50 mM, 300 mM, and 20 mM, respectively. Triton X-100 was added with an 1:100 ratio and mixed. The pH is adjusted to 8.0 with 5 M NaOH and sterilized by autoclaving for 15 min at 121 °C.

### Wash 2 Buffer

6.90 g  $\text{NaH}_2\text{PO}_4 \cdot \text{H}_2\text{O}$  , 17.54 g NaCl, and 3.4 g imidazole were dissolved in distilled water up to 1 L with a final concentrations of 50 mM, 300 mM, and 50 mM, respectively. Triton X-100 was added with an 1:100 ratio and mixed. The pH is adjusted to 8.0 with 5 M NaOH and sterilized by autoclaving for 15 min at 121 °C.

### Elution Buffer

6.90 g  $\text{NaH}_2\text{PO}_4 \cdot \text{H}_2\text{O}$  , 17.54 g NaCl, and 17 g imidazole were dissolved in distilled water up to 1 L with a final concentrations of 50 mM, 300 mM, and 250 mM, respectively. The pH is adjusted to 8.0 with 5 M NaOH and sterilized by autoclaving for 15 min at 121 °C.

**Table A.1** : The chemicals used in this study.

Chemicals	Company	Country
$\text{NaH}_2\text{PO}_4$	Merck	Germany
Imidazole	Merck	Germany
DTT	Applicem	Germany
TEMED	Sigma	Germany
Coomassie brilliant blue	Molecula	UK
Glycin	Sigma	Germany
APS	Molekula	UK
40% Acrylamide/Bis	BioRad	USA
Tris(hydroxymetyl)aminomethane; 99%	ABCR	Germany
NaCl	Merck	Germany
EDTA	Molekula	UK
$\text{MgCl}_2$	Merck	Germany

**Table A.1 (continued) :** The chemicals used in this study.

<b>Chemicals</b>	<b>Company</b>	<b>Country</b>
SDS	Molekula	UK
Acetic acid	Merck	Germany
Lysozyme	Fluka	Germany
Ampicilin	Roche	Switzerland
IPTG	Peqlab	Germany
PMSF	Molekula	UK
Glycerol	Merck	Germany
Ethanol	Merck	Germany
Methanol	Emboy	Turkey



## **APPENDIX B: Laboratory Equipments**

<b>Autoclave</b>	: Systec GmbH Labor-Systemtechnik, Germany
<b>Centrifuges</b>	: Beckman Coulter; Microfuge 18, USA; Beckman Coulter; AvantiJ30I, USA; Beckman Coulter, Allegra 25R Centrifuge, USA
<b>Deep freezers and refrigerators</b>	: -80°C New Brunswick Scientific, Ultra low Temperature Freezer, U410 Premium, USA; - 20°C and +4°C Arcelik Refrigerator, Turkey
<b>Ice Machine</b>	: Scotsman, AF 80, USA
<b>Laminar Flow Cabinet</b>	: Faster BH-EN2003, Italy
<b>Magnetic Stirrer</b>	: Heidolph Standard, Germany
<b>Orbital Shaker</b>	: Thermo Forma orbital shaker, USA
<b>Flat shaker</b>	: Heidolph, Duomax 1030, Germany
<b>pH meter</b>	: Mettler Toledo, Five Easy, Switzerland
<b>Micropipets</b>	: Eppendorf pipette, Germany
<b>Thermal Cycler</b>	: Applied Biosystems, GeneAmp, PCR System 2700, USA
<b>Vortex</b>	: Dragon Lab MX-F, China
<b>UV-Visible Spectrophotometer</b>	: Shimadzu UV-1700, Japan; Thermo Scientific, NanoDrop 2000 Spectrophotometer, USA
<b>Multiplate Spectrophotometer</b>	: BioRad Benchmark Plus, UK
<b>Water bath</b>	: Nüve, BM 302, Turkey
<b>Ultrasonicator</b>	: Bandelin, Sonoplus
<b>Ultrasonic bath</b>	: Elma, TranssonicTP690, Germany
<b>Balances</b>	: Precisa XB 220A, Switzerland; Precisa BJ610C, Switzerland



## **CURRICULUM VITAE**



**Name Surname:** Deniz Tanıl Yücesoy

**Place and Date of Birth:** Söke 1985

**Address:** MOBGAM-İTÜ

**E-Mail:** yucesoydeniz@gmail.com

**B.Sc.:** Izmir Institute of Technology, Department of Molecular Biology and Genetics

## **PUBLICATIONS/PRESENTATIONS ON THE THESIS**

- **Yucesoy, D.**, Cetinel, S., Caliskan, H.B., Yuca, E., Sarikaya, M., Karaguler, N.G., and Tamerler, C., 2011: Multifunctional Formate Dehydrogenase Fusion Protein Binds to Gold Surface with Improved Reaction Kinetics. *ICEST-2011 The International Conference on Enzyme Science and Technology*, October 31-November 4, Kusadasi, Turkey.
- **Yucesoy, D.**, Cetinel, S., Tamerler, C., 2011: The Utilization of GEPI-FDH Fusion Proteins in the Enzymatic Fuel Cells. *BMMP-11 International Symposium on Biomimetic Materials Processing*, January 25-28, Nagoya, Japan.